Biological Psychiatry

Multivariate Association between Functional Connectivity Gradients and Cognition in Schizophrenia Spectrum Disorders

--Manuscript Draft--

Manuscript Number:	BPS-D-24-00589
Full Title:	Multivariate Association between Functional Connectivity Gradients and Cognition in Schizophrenia Spectrum Disorders
Short Title:	Gradient-cognition associations in schizophrenias
Article Type:	Archival Report
Author Comments:	
Corresponding Author:	Ju-Chi Yu, Ph.D. Centre for Addiction and Mental Health Toronto, Ontario CANADA
Order of Authors:	Ju-Chi Yu, Ph.D.
	Colin Hawco, Ph.D.
	Lucy Bassman
	Lindsay D. Oliver, Ph.D.
	Miklos Argyelan, M.D.
	James M. Gold, Ph.D.
	Sunny X. Tang, M.D.
	George Foussias, M.D., Ph.D.
	Robert W. Buchanan, M.D.
	Anil K. Malhotra, M.D.
	Stephanie H. Ameis, M.D.
	Aristotle N. Voineskos, M.D., Ph.D.
	Erin W. Dickie, Ph.D.
Abstract:	Background Schizophrenia Spectrum Disorders (SSDs), which are characterized by social cognitive deficits, have been associated with dysconnectivity in “unimodal” (e.g., visual, auditory) and “multimodal” (e.g., default-mode and frontoparietal) cortical networks. However, little is known regarding how such dysconnectivity relates to social and non-social cognition, and how such brain-behavioral relationships associate with clinical outcomes of SSD. Methods We analyzed cognitive (non-social and social) measures and resting-state functional magnetic resonance imaging data from the ‘Social Processes Initiative in Neurobiology of the Schizophrenia(s) (SPINS)’ study (301 stable SSD and 185 healthy controls, ages 18-55). We extracted gradients from parcellated connectomes and examined the association between the first 3 gradients and the cognitive measures using partial least squares correlation (PLSC). We then correlated the PLSC dimensions with functioning and symptoms in the SSD group. Results The SSD group showed significantly decreased differentiation on all three gradients. The first PLSC dimension explained 67.39% ($p<.001$) of the covariance and showed a significant difference between SSD and controls (bootstrap $p<.05$). PLSC showed that

Powered by Editorial Manager® and ProduXion Manager® from Aries Systems Corporation

	all cognitive measures were associated with gradient scores of unimodal and multimodal networks (Gradient 1), auditory, sensorimotor, and visual networks (Gradient 2), and perceptual networks and striatum (Gradient 3), which were less differentiated in SSD. Furthermore, the first dimension was positively correlated with negative symptoms and functioning in SSD. Conclusions These results suggest a potential role of decreased differentiation of brain networks in cognitive and functional impairments in SSDs.
Additional Information:	
Question	**Response**
Have any of the data included in this submission already been published?	No
Number of words in the abstract	235
Number of words in the main text	3960
Number of tables (main-text only)	3
Number of figures (main-text only)	4
Number of supplemental files	1
Suggested Reviewers:	Daniel S. Margulies, Ph.D. Associate professor, University of Paris daniel.margulies@cnrs.fr
	Bratislav Misic, Ph.D. Associate professor, McGill University bratislav.misic@mcgill.ca
	Roscoe O. Brady, M.D., Ph.D. Associate Professor, Havard Medical School robrady@bidmc.harvard.edu
	Paul E. Croarkin, D.O., M.S. Professor, Mayo Clinic School of Medicine croarkin.paul@mayo.edu
	Adrienne C. Lahti, M.D. Professor, The University of Alabama at Birmingham alahti@uab.edu
	Deepak K. Sarpal, M.D. Associate professor, University of Pittsburgh sarpaldk@upmc.edu
Opposed Reviewers:	
Keywords:	functional connectivity; schizophrenia spectrum disorders; social cognition; principal gradient analysis; partial least squares correlation; fMRI

Powered by Editorial Manager® and ProduXion Manager® from Aries Systems Corporation

camh

April 15th, 2024

Dear Dr. Krystal,

Please consider our manuscript, entitled “Multivariate Association between Functional Connectivity Gradients and Cognition in Schizophrenia Spectrum Disorders” for consideration as an Archival Report in *Biological Psychiatry*.

Schizophrenia spectrum disorders (SSDs) are characterized by cognitive deficits relating to dysconnectivity between unimodal and multimodal networks. However, little is known regarding how such connectivity relates to social and non-social cognitive performance specifically in SSDs, and how such brain-behavior relationship contributes to the daily life of participants with SSDs. We used harmonized data from the National Institute of Mental Health (NIMH)-funded “Social Processes Initiative in the Neurobiology of Schizophrenia(s) (SPINS)” multicenter study, where multimodal data were collected from 185 healthy controls and 301 participants with SSDs. We first extracted principal gradients from resting-state connectivity data to characterize their functional network organization and used partial least squares correlation (PLSC) to examine its multivariate association with both social and non-social cognitive performance. We then examined the clinical relevance of such brain-behavior relationships by examining the correlation between the identified PLSC dimension and clinical and functioning outcomes of participants with SSDs.

Our results showed that participants with SSDs featured less network segregation along the unimodal-multimodal gradient, the visual-sensorimotor gradient, and the default-frontoparietal gradient. Such segregations were associated with social and non-social cognition, and these associations were shown clinically meaningful as they correlated with participants symptoms, quality of life, and functioning in SSDs. We believe this study holds relevance for the diverse readership of *Biological Psychiatry*, offering insights into the nature and mechanisms of psychiatric disorders by illuminating potential prognostic markers associated with SSDs.

Suggested reviewers: Daniel S. Margulies (daniel.margulies@cnrs.fr)
Bratislav Misic (bratislav.misic@mcgill.ca)
Roscoe O. Brady (robrady@bidmc.harvard.edu)
Paul E. Croarkin (croarkin.paul@mayo.edu)
Adrienne C. Lahti (alahti@uab.edu)
Deepak K. Sarpal (sarpaldk@upmc.edu)

I affirm that this manuscript is an original, unpublished study that has not been submitted for simultaneous consideration by any other journal. The authors have no potential conflicts of interest to disclose.

Sincerely,

Ju-Chi Yu, Ph.D. & Erin W. Dickie, Ph.D.
Centre for Addiction and Mental Health
250 College Street, Toronto, ON, Canada M5T 1R8
E-mail: Ju-Chi.Yu@camh.ca, Erin.Dickie@camh.ca

Multivariate Association between Functional Connectivity Gradients and Cognition in Schizophrenia Spectrum Disorders

Authors
Ju-Chi Yu[1], Colin Hawco[1,2], Lucy Bassman[1], Lindsay D. Oliver[1,2], Miklos Argyelan[3], James M. Gold[4], Sunny X. Tang[3], George Foussias[1,2], Robert W. Buchanan[4], Anil K. Malhotra[3], Stephanie H. Ameis[1,2], Aristotle N. Voineskos[1,2]*, Erin W. Dickie[1,2]*

1.Kimel Family Translational Imaging-Genetics Research Lab, Campbell Family Mental Health Research Institute, Centre for Addiction and Mental Health, Toronto, Canada;
2. University of Toronto, Temerty Faculty of Medicine, Department of Psychiatry, Toronto, Canada
3. Zucker Hillside Hospital, Glen Oaks, NY, USA;
4. Maryland Psychiatric Research Center, Department of Psychiatry, University of Maryland School of Medicine, Baltimore, MD, USA.

Corresponding authors: Ju-Chi Yu (Ju-Chi.Yu@camh.ca); Erin W. Dickie (Erin.Dickie@camh.ca)

Running title: Gradient-cognition associations in schizophrenias
Keywords: principal gradient analysis, schizophrenia spectrum disorders, social cognition, functional connectivity, partial least squares correlation, fMRI

Number of Words in abstract: 235
Number of Words: 3960
Number of Figures: 4
Number of Tables: 3

Abstract

Background: Schizophrenia Spectrum Disorders (SSDs), which are characterized by social cognitive deficits, have been associated with dysconnectivity in "unimodal" (e.g., visual, auditory) and "multimodal" (e.g., default-mode and frontoparietal) cortical networks. However, little is known regarding how such dysconnectivity relates to social and non-social cognition, and how such brain-behavioral relationships associate with clinical outcomes of SSD.

Methods: We analyzed cognitive (non-social and social) measures and resting-state functional magnetic resonance imaging data from the 'Social Processes Initiative in Neurobiology of the Schizophrenia(s) (SPINS)' study (301 stable SSD and 185 healthy controls, ages 18-55). We extracted gradients from parcellated connectomes and examined the association between the first 3 gradients and the cognitive measures using partial least squares correlation (PLSC). We then correlated the PLSC dimensions with functioning and symptoms in the SSD group.

Results: The SSD group showed significantly decreased differentiation on all three gradients. The first PLSC dimension explained 67.39% ($p<.001$) of the covariance and showed a significant difference between SSD and controls (bootstrap $p<.05$). PLSC showed that all cognitive measures were associated with gradient scores of unimodal and multimodal networks (Gradient 1), auditory, sensorimotor, and visual networks (Gradient 2), and perceptual networks and striatum (Gradient 3), which were less differentiated in SSD. Furthermore, the first dimension was positively correlated with negative symptoms and functioning in SSD.

Conclusions: These results suggest a potential role of decreased differentiation of brain networks in cognitive and functional impairments in SSDs.

Introduction

Schizophrenia spectrum disorders (SSDs) are characterized by positive, negative, and general psychopathology symptoms, as well as deficits in social and non-social cognition that affect daily life. Two prior studies found consistent network segregation patterns in SSDs characterized by dysconnectivity in "unimodal" (e.g., visual, auditory) and "multimodal" (e.g., default mode, frontoparietal) cortical networks (1,2). Such changes in cortical network configuration can be explored using an emerging technique known as principal gradient analysis, which is a data reduction method used to characterize participants' brain connectivity profiles (3). This approach provides a topographical representation of functional connectivity and network organization by extracting principal gradients (i.e., a type of latent dimension) from a participant's brain connectivity pattern and identifying the dominant network segregation patterns from each gradient.

Human behaviors and cognitions are often generated from the coordinated functioning of different brain regions (4), which is closely linked to the geometry of brain (5). By integrating geodesic features, gradient analysis generates hierarchical levels in brain network organizations that map onto different levels of cognition, and has been used to examine how functional connectivity relates to cognition; e.g., creativity performance (6) and semantic cognition (7,8), where the neurocognitive system of semantic cognition was found to also regulate social cognition (9). By using such gradient technique to examine functional connectivity of SSDs, recent studies found that, compared to controls, people with SSDs feature less distinct unimodal-multimodal (1,10,11) and visual-sensorimotor (1,12) network segregations; because the decreased segregation is represented by networks moving toward the center from both ends of the gradient axes, it is termed 'gradient compression.' In these studies, the gradient compression on the unimodal-multimodal axis was found to correlate with clinical symptoms (1,11) and lower processing speed (11). As people with SSDs vary extensively in symptoms (13), treatment response (14,15), cognition (16,17), and brain activity (18–20), gradient analysis provides a general principle of quantifying functional brain organization to investigate individual differences in brain configurations of SSD while accounting for heterogeneous brain features, which relate to treatment responses (21) and psychotic symptoms (1,11,21) of people with SSDs.

Social and non-social cognition are critically important to functioning in people with SSDs (22). Recent work by our group suggests that non-social cognitive performance, and particularly social cognitive performance may relate to network segregation in people with SSDs (2,20). With a large sample of participants measured on social and non-social cognition, application of gradient analysis may help further our understanding of how network segregation relates to these two aspects of cognitive deficits in SSDs. As social and non-social cognition are strongly related to functional outcomes (2,21,23,24), further examination on brain gradient-cognitive relationships can reveal how such relationships influence individual differences in the functional outcomes in SSDs.

To examine brain gradient-cognitive relationships, we used data from the National Institute of Mental Health (NIMH)-funded "Social Processes Initiative in the Neurobiology of Schizophrenia(s) (SPINS)" multicenter study (24). These harmonized data included functional brain imaging and comprehensive assessments of both social and non-social cognition. To account for inter-assessment associations and maximize statistical power, we examined brain-

behavior relationships with a multivariate approach, which extracts latent dimensions that identify the dominant association between large sets of variables. The individual differences within associations were then used to examine how brain-behavior relationships manifest individual differences in functioning. In addition to replicating prior findings of gradient compression in SSDs, we specifically aimed to 1) identify the gradients that are associated with social and non-social cognition, and 2) examine how such associations contribute to clinical outcomes, including functioning, quality of life, and clinical symptoms in people with SSDs.

Methods and Materials

Participants

In total, 301 participants with SSDs and 185 Controls were recruited for the SPINS study (24). The diagnoses of SSDs (i.e., schizophrenia, schizoaffective disorder, schizophreniform disorder, delusional disorder, and psychotic disorder) were based on the DSM-5 as assessed by the Structured Clinical Interview for DSM (SCID-IV-TR). All participants with SSDs had no changes in antipsychotic medication or functioning/support level for 30 days before enrollment. Participants were excluded if they had a history of head trauma, substance use disorder, intellectual disability, unstable medical illness, or other neurological diseases. Controls were excluded if they had any lifetime Axis I psychiatric disorder (except adjustment disorder, phobic disorder, and past major depression with 2+ years remission and currently unmedicated) or a first-degree relative with a psychotic disorder. Chlorpromazine (CPZ) equivalents were calculated for the 222 participants with SSDs based on available medication information (25). All participants provided informed consent; the research followed the Declaration of Helsinki and was approved by relevant ethics and institutional review boards.

Demographics, Cognitive, and Clinical Assessment

Premorbid IQ was estimated by the Wechsler Test of Adult Reading (WTAR) (26). Psychiatric symptoms in SSDs were evaluated using the Brief Psychiatric Rating Scale (BPRS) (27) and Scale for the Assessment of Negative Symptoms (SANS) (28,29). Functional outcomes were assessed using the Birchwood Social Functioning Scale (BSFS) (30) and Quality of Life Scale (QLS) (31).

The study collected a comprehensive battery of non-social and social cognitive measures that have previously been described in detail (24,32). Non-social cognition was assessed using the 6 domain scores of the MATRICS (Measurement and Treatment Research to Improve Cognition in Schizophrenia) Consensus Cognitive Battery (MCCB) (33): processing speed, reasoning/problem solving, attention/vigilance, working memory, verbal learning, and visual learning. The social cognitive battery included the Penn Emotion Recognition Test (ER40) (34), Reading the Mind in the Eyes Test (RMET) (35), and The Awareness of Social Inference Test – Revised (TASIT) (36), which included three sub-tests: TASIT 1, identifying emotions; TASIT 2 minimal social inferences including sincere, simple sarcasm, and paradoxical sarcasm; and TASIT 3 measuring social inferences (lies and sarcasm) with enriched contextual cues. These 14 cognitive variables (including ER40 total, RMET total, TASIT 1 total, 3 subscores from TASIT 2, 2 subscores from TASIT 3, and the 6 domain scores from MCCB) were used as cognitive data to examine associations with the principal gradients.

MRI Data Acquisition and Quality Control

Multimodal MRI scans were obtained using 3T scanners with multichannel head coils (see **Supplementary Material**). Anatomical T1-weighted scans were collected using a fast-gradient sequence (0.9mm isotropic voxels, see supplemental for site specific parameters). Resting-state scan was a 7-minute EPI sequence (TR=2000 ms, TE=30 ms, flip angle=77°, field of view=20°, in-plane resolution=3.125 mm^2, and slice thickness=4 mm). Participants were instructed to let their mind wander with their eyes closed.

All scans were quality checked before and after being preprocessed by fMRIPrep 1.5.8 (37) and ciftify 2.3.1 (38) workflows. From the preprocessing, all scans were performed nuisance regression to correct for head motion, white matter signal, cerebral spinal fluid signal, and the global signal (see details for imaging preprocessing in **Supplementary Material**). Participants with excessive motion (mean framewise displacement>0.5 mm) were excluded from further analysis (see **Figure S1**).

Connectivity Matrix Construction

To construct connectivity matrices, we parcellated the brain using the cortical Multimodal Parcellation (39) atlas (360 regions) and the Melbourne Subcortex Atlas (40) with all cortical regions categorized into twelve networks according to the Cole-Anticevic Brain Network Parcellation (41) (see **Figure 1A**), with the subcortical regions grouped separately. For each participant, a 392 × 392 functional connectivity matrix was created via the Fisher *Z*-transformation of the Pearson's correlation of the time-series from each parcel. Finally, we used the neuroCombat R package to perform ComBat, a batch-effect correction, on the *Z*-transformed connectivity to harmonize the connectivity data across 6 MRI scanners (42,43).

Network Hierarchy Measures: Gradient Analysis

To quantify network hierarchy, gradient analysis uses a dimension reduction approach to extract principal gradients from a brain connectivity matrix. In the procedure, the data were transformed back to Pearson correlation coefficients after ComBat, and the data for each participants underwent diffusion map embedding (44) using the *BrainSpace* package (45) to extract principal gradients (3). These gradients capture specific network segregations that contribute to the overall functional connectivity pattern. Gradients are ordered such that they contribute to the total variance in a descending order. Principal gradients also account for geodesic features between brain regions – i.e., given the assumption that two closer brain regions are more likely to be functionally connected, the geodesic features are accounted for such that two regions that are physically closer are also more likely to be closer in values on these gradients. To allow comparisons between gradients across participants, we aligned them via Procrustean rotation with a template gradient map (3). This gradient map reveals the three gradients shown in **Figure 1B-C**. The ROIs are represented by scores on each gradient, and these gradient scores are averaged across brain networks to illustrate the representations of these networks on these gradients. As expected, the first gradient differentiates connectivity between the unimodal networks (e.g., primary and secondary visual (VIS1 and VIS2), auditory (AUD), and somatomotor (SMN) networks) from the multimodal networks (e.g., default mode (DMN), frontoparietal (FPN), and language (LAN) networks). The second gradient further differentiates connectivity within the unimodal networks (i.e., VIS1 and VIS2 vs. AUD and SMN), and the third gradient differentiates within the multimodal networks (i.e., DMN and LAN vs. FPN and cingular opercular network (CON)). This gradient analysis was performed with Python 3.8.6-GCCcore-10.2.0. Distributions of eigenvalues of all extracted gradients are shown in **Figure S2** to illustrate the variance explained by each gradient.

Statistical Analyses

We examined group differences between participants with SSDs and controls in demographics and cognition with two-sample *t*-tests (or equivalent tests to account for non-normally distributed or heterogeneous data; see **Supplementary Material**). Group differences (SSD-control) in

gradient scores were also examined with two-sample *t*-tests using the linear model approach (i.e., the *lm* function in R) and were corrected for multiple comparisons with a false discovery rate (FDR) approach (q<.05). From the linear model, we report the number (n) of significant ROIs of each network with their range of *F*-statistics.

Multivariate associations between the cognitive and network hierarchy measures across SSD and control groups were then analyzed by partial least squares correlation (PLSC) (46), relating 14 cognitive variables (8 social cognitive scores and 6 MCCB domain scores) to 1176 brain variables (gradient scores of the first 3 dimensions of 392 brain regions). Age, sex, and mean framewise displacement (FD) were regressed out from all behavior and brain measures prior to PLSC. In PLSC, each variable is centered (i.e., having a mean of 0) and normalized (such that the sum of squared values equals 1). PLSC then extracts, from their cross product, latent dimensions, which are analogous to components in principal component analysis (PCA), explaining associations between the brain and cognitive measures. On each dimension, PLSC generates pairs of latent variables, analogous to factor scores in PCA; consisting of one computed from the cognitive variables (i.e., *cognitive scores*) and one from the brain variables (i.e., *brain scores*), which together have maximum covariance. Significance of PLSC dimensions was assessed via permutation tests (47), while bootstrap tests (48) were used to examine the stability of the loadings for each variable. From both tests, we derived *p* values to indicate significant differences. Additionally, the bootstrap test gives a *Z*-analogous statistic called bootstrap ratio (BR), of which a value of 2.88 is associated with a *p* of .005. This allows identification of variables which significantly contribute to each dimension. The effect sizes of variables were quantified by their contributions, computed as squared loadings, to determine the importance of each variable to each dimension. See **Supplementary Material** for further details.

To examine the clinical representation of PLSC results, we performed Pearson correlation tests within the SSD sample between the brain and the cognitive scores from PLSC and all subscores of the symptom and functioning measures. Participants with missing values were removed from related analyses. Results were FDR-corrected for 8 comparisons with q<.05. All data analyses were performed using R 4.1.1 (49) with PLSC being performed using the *TExPosition* and the *data4PCCAR* packages (https://github.com/HerveAbdi/data4PCCAR).

Results

Demographics and Behavioral Characteristics

After quality control (detailed in **Figure S1**), the data analysis included 248 participants with SSDs (M_{age}=31.42, SD_{age}=9.77, 79 females) and 172 Controls (M_{age}=31.95, SD_{age}=10.40, 80 females). Participant characteristics and cognitive test scores are shown in **Table 1**. Two-sample *t*-tests showed no significant age difference between the SSD and the Control groups. SSD had lower mean scores than Controls for all cognitive measures except TASIT 2 sincere videos, consistent with prior findings (2,32) (See **Table 1**).

Decreased Differentiation Across all Three Gradients in SSDs vs. Controls

The significant group differences in gradients across brain regions are shown in **Figure 2A** and illustrated by arrows representing each region of interest (ROI) in **Figure 2B-2D** pointing from the mean gradient scores of Controls to those of the SSD group. Overall, participants with SSDs showed decreased differentiations at FDR-corrected α=0.05 along all three gradients. Specifically, on Gradient 1 (unimodal vs. multimodal), somatomotor (SMN), primary and secondary visual (VIS1 and VIS2), and default mode networks (DMN) are found to be less differentiated from auditory (AUD), cingulo-opercular (CON), frontoparietal (FPN), and subcortical (SUB) networks in participants with SSDs than in Controls, q<.05. Although participants with SSDs have reliably higher gradient scores compared to Controls for ROIs from the default mode network (DMN), these ROIs have different patterns from those of the other networks. Descriptively, the ROIs from other networks showed decreased differentiation between networks for participants with SSDs, whereas the ROIs from DMN showed decreased differentiation within the network for participants with SSDs, as indicated by red arrows moving towards each other or the mean scores in **Figures 2B-2D**, **S3** and **S4**. On Gradient 2 (visual vs. auditory), the SSD group has less differentiation of CON, SUB, SMN, AUD, and FPN from dorsal attention (DAN), VIS1, and VIS2, q<.05. Similar to Gradient 1, we also see decreased within-network differentiation in DMN (see **Figures S3** and **S4**). On Gradient 3 (default vs. frontoparietal), the SSD group showed decreased differentiation of CON and SUB from DAN, VIS1, VIS2, and language (LAN) networks, q<.05. Detailed statistics are reported in **Table 2** with ranges of significant F statistics and numbers of significant ROIs of each network.

Multivariate analysis of cognitive-network hierarchy PLSC reveals a significant dimension, whereby networks with decreased differentiation relate to cognitive performance

PLSC analysis identified one significant dimension, as determined by permutation test (p<.001), explaining 67.4% of the cognition-gradient covariance. This dimension features the general correlations between all cognitive measures (both social and non-social; **Figure 3A**) and network hierarchy (**Figure 3B**). The loadings in **Figure 3A** show that all cognitive measures contribute similarly (i.e., in the same direction). In this dimension, participants with SSDs and Controls are significantly different according to a bootstrap test both in brain and in cognitive scores as indicated by non-overlapping 95% bootstrap confidence intervals of their means (**Figure 3C**).

As Dimension 1 differentiates participants with SSDs from Controls, to better illustrate the PLSC results of network hierarchy, we plotted the group differences of each ROI in Figures **3D-3F** (similar to **Figures 2B-2D**) and highlighted those that contributed reliably (BR>2.88, p<.005).

Overall, this network hierarchy–cognition association, identified by the first dimension of PLSC, is driven by contributing ROIs, which also happened to show decreased differentiation along all three gradients. For instance, PLSC identified ROIs from SMN, VIS2, DMN and Thalamus, which in SSD showed decreased differentiations on Gradient 1 (unimodal vs. multimodal networks). For Gradient 2 (visual vs. auditory networks), PLSC identified ROIs from CON, AUD, SMN, FPN, VIS2, and DAN, where the decreased differentiations of SSD were found mainly between different perceptual networks; more specifically, between AUD, SMN, FPN, CON and VIS2 with DAN. For Gradient 3 (default vs. frontoparietal networks), PLSC identified ROIs from the perceptual, language, and subcortical networks, where decreased differentiations of SSD were found between the unimodal networks (i.e., VIS and SMN) and LAN versus SUB.

Given the heterogeneity of ROIs in the DMN, it is worth noting that these identified DMN ROIs identified for Gradient 1 are those that are located closer to the visual networks. On Gradient 2, the identified ROIs within DMN were those medial regions closer to FPN and temporal regions closer to VIS. Interestingly, the identified ROIs of Gradient 3 from SMN, CON, and AUD networks were also those that were close to LAN.

The first PLSC dimension is significantly related to functioning via both brain scores and cognitive scores

From the SSD group, the correlation between the first latent variables (i.e., the behavior and the brain scores) and the clinical assessments of functioning or symptoms are illustrated in **Figure 4**. **Figure 4A** shows that, for Dimension 1, the cognitive scores are negatively correlated with the total score of BSFS (r=-.19, df=246, CI=[-.31, -.07], q=.0029) and total scores of QLS (r=-.33, df=244, CI=[-.44, -.22], q<.0001), positively correlated with the SANS total score (r=.23, df=244, CI=[.11, .35], q=.0003), but have no significant correlation with symptoms on the BPRS total score (r=.12, df=246, CI=[.0003, .25], q=.0564). These correlations remained significant after controlling for CPZ dosage equivalent (**Table S1**).

Similarly, the brain scores of this dimension are negatively correlated with functioning, including the BSFS (r=-.25, df=246, CI=[-.36, -.13], q=.0002) and QLS (r=-.28, df=244, CI=[-.39, -.16], q<.0001, two missing values) total scores. However, these brain scores are positively correlated only with the SANS total score (r=.24, df=244, CI=[.12, .36], q=.0002), but not general psychopathology as measured by the BPRS total score (r=.11, df=246, CI=[-.01, .23], q=.0753). Correlation results with individual subscales are detailed in **Table 3** and **Figure 4B**.

Discussion

This study examined gradients from the resting-state functional connectivity of SSDs and Controls, using PLSC to explore multivariate associations with social and non-social cognition. Gradients offer an advantage of prior work focused on functional connectivity strength, as the gradient analysis considers topographical properties of how the brain networks are organized (e.g., in terms of well or poor segregation between unimodal and multimodal networks). With a well-powered sample, we successfully replicated prior findings of unimodal-multimodal (Gradient 1) (1,10,11) and visual-sensorimotor (Gradient 2) (12) gradient compressions in SSDs and extended those findings via a compression of Gradient 3 between different multimodal networks. The PLSC results revealed the association between compressions along three gradients and the group differences between SSDs and Controls in both social and non-social cognitive abilities. Finally, in the SSD group, the identified brain-cognition dimension was found correlated with clinical symptoms and functional outcomes with higher latent cognitive and brain scores correlated with higher negative symptoms and lower functioning and quality of life. Overall, by combining this rich brain, behavioral, and functioning data with advanced multivariate methods, we identified how changes in the underlying properties of brain network organization, specifically decreased differentiation of canonical networks, relates to cognitive impairments in SSDs, and ultimately psychopathology and functioning.

In contrast to previous gradient studies in SSD (1,11,12), we included a broad assessment of social cognitive measures and examined multivariate associations with network organization. Although PLSC does not differentiate social from non-social cognition in brain-behavioral associations, the results were not a surprise as non-social and social cognitive performance are correlated and depend on overlapping networks (2,22). Our study showed that the differences in general cognitive ability between participants with SSDs and Controls are most related to the compression between the networks of vision (VIS1 and VIS2) and CON, along with other sensory modalities (AUD and SMN). These results are similar to Dong et al. (1) and Holmes et al. (12) and could be related to atypical connectivity especially in the visual and auditory networks (50), which give rise to positive symptoms or changes in cognition (51). Furthermore, from Dimension 1 of our PLSC, we identified associations between cognition and decreased distinctions of two other areas: 1) between striatum and LAN on Gradient 3 and 2) between thalamus and unimodal networks on Gradient 1. These findings are consistent with increased thalamic-sensorimotor connectivity in previous literature (52–54) and support the hypothesis proposed by Andreasen et al. (55) that the dysfunction of the cortical-subcortical-cerebellar circuit (with thalamus being one of the main nodes) contributes to symptoms and cognitive deficits in SSDs. In addition, the contributing subcortical ROIs identified on Gradient 3 include caudate and nucleus accumbens, of which the connectivity to cortical regions were also found associated with improving psychosis after treatments for participants with first-episode SSDs (21).

Similar gradient compression has been shown in other populations and disorders, such as aging (56), sleep deprivation (57), usage of lysergic acid diethylamide (49), and to other psychiatric disorders, such as major depressive disorder (18) and autism spectrum disorder (ASD; 60). With similar cognitive challenges, SSDs and autism feature similar gradient compression, but different regions affected were found, which may relate to the difference between their symptom manifestation and onset time. Specifically for autism, another heterogenous disorder, Choi et al. (60) showed that only the most severe of three delineated subgroups featured gradient

compression. Similar compression to SSDs was found in autism for sensorimotor regions, anterior cingulate cortex (ACC), visual cortex, and right inferior temporal cortex (ITC), where ACC and ITC were associated with semantic control and social cognition (9). Their study found compression in autism in the posterior cingulate cortex but not in the auditory network, which was found in our study, suggesting that disorder-specific functional brain organizations could exist.

Previous studies have shown the alignment between principal gradients and human microstructural gradients of brain regions and the T1/T2 myelination map (61–63). A significant proportion of gene sets that show differential expression across the myelination map are also shown associated with SSDs (64). As a result, the identified gradient compression of SSDs could be related to myelin abnormalities. As SSDs tend to present clinically while myelination is in progress, a "demyelination hypothesis" of SSDs has been proposed (65). Recently, decreased cortical myelination has been found in people with SSDs (65,66) encompassing inferior longitudinal fasciculus (ILF) and superior longitudinal fasciculus (SLF) (66). Between them, ILF connects temporal and occipital cortices, which align with the two ends of the visual-sensorimotor gradient, and SLF connects frontal and occipital cortices, which align with the two ends of the unimodal-multimodal gradient. Therefore, the observed visual-sensorimotor and unimodal-multimodal gradient compressions could be related to the disruption of myelination in these white matter tracts, ILF and SLF respectively, which connect those networks.

These results provide insights into the network mechanisms of SSDs but also have some sample characteristics that may influence the nature of our results. Participants with SSDs in the SPINS data set were on stable antipsychotic treatment. Although our correlation analysis replicated previous literature on the absence of an association between network compression and positive symptoms, this result could be influenced by examination of a clinically stable sample. Antipsychotic medication has also been shown to impact brain structure (67), though the effects on gradients are unknown - we regressed out CPZ equivalents to help address this issue. Furthermore, though site and motion effects were present in our data, they were mitigated using harmonization by statistical regression, and preprocessing workflows and quality checks, respectively. In addition, although our study only includes SSDs, the observed results could relate to general risk of mental health and future studies expanding into transdiagnostic samples is worthwhile.

The majority of prior work examining connectivity in SSDs and relation to cognition largely focused on the strength of specific connections (24,53,68). Gradients analysis allows exploration of broader changes in the organizational structure of these networks across individuals (3,56). Specifically, we found that reduced segregation across networks is associated with psychopathology and weaker performance in social and non-social cognition, which in turn predicts functional outcomes. We therefore propose that cognitive deficits in SSDs are not driven only by 'reduced' connectivity, but deficits in the organizational structure of canonical brain networks and consequent reductions in network segregation. The correlations within SSDs to clinical symptoms and functional outcomes demonstrates that these associations between gradients and cognition were clinically meaningful. These results provide insights into the mechanisms of brain organization underlying cognitive impairment and behavioral outcomes across individuals with SSDs, and may serve as prognostic markers and potential treatment targets moving forward.

Acknowledgement

The authors would like to thank all participants for their contribution to this work, and the research staff who performed data collection and management. This work was supported by National Institute of Mental Health grants 1/3R01MH102324–01 (to Dr. Voineskos), 2/3R01MH102313–01 (to Dr. Malhotra), and 3/3R01MH102318–01 (to Dr. Buchanan) as well as support from the Discovery Fund of the Centre for Addiction and Mental Health (CAMH) and the Canadian Institutes of Health Research (CIHR).

Conflict of Interest Disclosures

J-CY receives grant support from the Discovery Fund of the Centre for Addiction and Mental Health (CAMH). CH receives grant support from the National Institute of Mental Health (NIMH), Canadian Institutes of Health Research (CIHR), and the Centre for Addiction and Mental Health (CAMH) Foundation. LB reported no biomedical financial interests or potential conflicts of interest. LDO receives grant support from the Brain & Behavior Research Foundation (BBRF). MA reported no biomedical financial interests or potential conflicts of interest. JMG has no conflict of interest to declare. SXT receives grant support from the NIMH (K23 MH130750, R21 AG082054), she also owns equity and serves as a consultant for North Shore Therapeutics, received research funding and serves as a consultant for Winterlight Labs, and is on the advisory board and owns equity for Psyrin. GF currently receive funding from CIHR, the CAMH Foundation, and the University of Toronto. RWB has consulted for Boehringer-Ingelheim, serves on the Data Safety and Monitoring Boards of Roche, Merck, and Newron, and has served on the Advisory Boards of Merck, Acadia, Karuna, and Neurocrine. AKM receives grant support from the NIMH (R01 MH109508, R01 MH108654, R61 MH120188). SHA currently receives funding from the NIMH (R01 MH114879), CIHR, University of Toronto, and the CAMH Foundation. ANV currently receives funding from the NIMH (1/3R01 MH102324, 1/5R01 MH114970), CIHR, Canada Foundation for Innovation, CAMH Foundation, and University of Toronto. EWD has received funding from BBRF, NIMH, CIHR, and CAMH Foundation. The funding organizations had no role in the design and conduct of the study; collection, management, analysis, and interpretation of the data; preparation, review, or approval of the manuscript; and decision to submit the manuscript for publication.

References

1. Dong D, Yao D, Wang Y, Hong S-J, Genon S, Xin F, *et al.* (2021): Compressed sensorimotor-to-transmodal hierarchical organization in schizophrenia. *Psychol Med* 1–14.
2. Oliver LD, Hawco C, Homan P, Lee J, Green MF, Gold JM, *et al.* (2021): Social Cognitive Networks and Social Cognitive Performance Across Individuals With Schizophrenia Spectrum Disorders and Healthy Control Participants. *Biol Psychiatry Cogn Neurosci Neuroimaging* 6: 1202–1214.
3. Margulies DS, Ghosh SS, Goulas A, Falkiewicz M, Huntenburg JM, Langs G, *et al.* (2016): Situating the default-mode network along a principal gradient of macroscale cortical organization. *Proc Natl Acad Sci* 113: 12574–12579.
4. Park H-J, Friston K (2013): Structural and Functional Brain Networks: From Connections to Cognition. *Science* 342: 1238411.
5. Pang JC, Aquino KM, Oldehinkel M, Robinson PA, Fulcher BD, Breakspear M, Fornito A (2023): Geometric constraints on human brain function. *Nature* 618: 566–574.
6. Huo T, Xia Y, Zhuang K, Chen Q, Sun J, Yang W, Qiu J (2022): Linking functional connectome gradient to individual creativity. *Cereb Cortex N Y N 1991* bhac013.
7. Gao Z, Zheng L, Krieger-Redwood K, Halai A, Margulies DS, Smallwood J, Jefferies E (2022): Flexing the principal gradient of the cerebral cortex to suit changing semantic task demands. *eLife* 11: e80368.
8. Gonzalez Alam TRDJ, Mckeown BLA, Gao Z, Bernhardt B, Vos De Wael R, Margulies DS, *et al.* (2022): A tale of two gradients: differences between the left and right hemispheres predict semantic cognition. *Brain Struct Funct* 227: 631–654.
9. Diveica V, Koldewyn K, Binney RJ (2021): Establishing a role of the semantic control network in social cognitive processing: A meta-analysis of functional neuroimaging studies. *NeuroImage* 245: 118702.
10. Dong D, Luo C, Guell X, Wang Y, He H, Duan M, *et al.* (2020): Compression of Cerebellar Functional Gradients in Schizophrenia. *Schizophr Bull* 46: 1282–1295.
11. Wang M, Li A, Liu Y, Yan H, Sun Y, Song M, *et al.* (2020): *Reproducible Abnormalities of Functional Gradient Reliably Predict Clinical and Cognitive Symptoms in Schizophrenia*. Neuroscience. https://doi.org/10.1101/2020.11.24.395251
12. Holmes A, Levi PT, Chen Y-C, Chopra S, Aquino KM, Pang JC, Fornito A (2023): Disruptions of Hierarchical Cortical Organization in Early Psychosis and Schizophrenia. *Biol Psychiatry Cogn Neurosci Neuroimaging* S2451902223002203.
13. Tsuang MT, Lyons MJ, Faraone SV (1990): Heterogeneity of Schizophrenia: Conceptual Models and Analytic Strategies. *Br J Psychiatry* 156: 17–26.
14. Conley RR, Kelly DL (2001): Management of treatment resistance in schizophrenia. *Biol Psychiatry* 50: 898–911.
15. Leucht S, Cipriani A, Spineli L, Mavridis D, Örey D, Richter F, *et al.* (2013): Comparative efficacy and tolerability of 15 antipsychotic drugs in schizophrenia: a multiple-treatments meta-analysis. *The Lancet* 382: 951–962.
16. Goldstein G, Allen DN, Van Kammen DP (1998): Individual Differences in Cognitive Decline in Schizophrenia. *Am J Psychiatry* 155: 1117–1118.
17. Van Rheenen TE, Lewandowski KE, Tan EJ, Ospina LH, Ongur D, Neill E, *et al.* (2017): Characterizing cognitive heterogeneity on the schizophrenia–bipolar disorder spectrum. *Psychol Med* 47: 1848–1864.
18. Gallucci J, Pomarol-Clotet E, Voineskos AN, Guerrero-Pedraza A, Alonso-Lana S, Vieta E, *et al.* (2022): Longer illness duration is associated with greater individual variability in functional brain activity in Schizophrenia, but not bipolar disorder. *NeuroImage Clin* 36: 103269.
19. Gallucci J, Tan T, Schifani C, Dickie EW, Voineskos AN, Hawco C (2022): Greater individual variability in functional brain activity during working memory performance in Schizophrenia Spectrum Disorders (SSD). *Schizophr Res* 248: 21–31.

20. Hawco C, Buchanan RW, Calarco N, Mulsant BH, Viviano JD, Dickie EW, *et al.* (2019): Separable and Replicable Neural Strategies During Social Brain Function in People With and Without Severe Mental Illness. *Am J Psychiatry* 176: 521–530.
21. Sarpal DK, Robinson DG, Lencz T, Argyelan M, Ikuta T, Karlsgodt K, *et al.* (2015): Antipsychotic Treatment and Functional Connectivity of the Striatum in First-Episode Schizophrenia. *JAMA Psychiatry* 72: 5.
22. Fett A-KJ, Viechtbauer W, Dominguez M-G, Penn DL, Van Os J, Krabbendam L (2011): The relationship between neurocognition and social cognition with functional outcomes in schizophrenia: A meta-analysis. *Neurosci Biobehav Rev* 35: 573–588.
23. Argyelan M, Gallego JA, Robinson DG, Ikuta T, Sarpal D, John M, *et al.* (2015): Abnormal Resting State fMRI Activity Predicts Processing Speed Deficits in First-Episode Psychosis. *Neuropsychopharmacology* 40: 1631–1639.
24. Viviano JD, Buchanan RW, Calarco N, Gold JM, Foussias G, Bhagwat N, *et al.* (2018): Resting-State Connectivity Biomarkers of Cognitive Performance and Social Function in Individuals With Schizophrenia Spectrum Disorder and Healthy Control Subjects. *Biol Psychiatry* 84: 665–674.
25. Leucht S, Samara M, Heres S, Davis JM (2016): Dose Equivalents for Antipsychotic Drugs: The DDD Method. *Schizophr Bull* 42: S90–S94.
26. Wechsler D (2001): *Wechsler Test of Adult Reading: WTAR.* Psychological Corporation.
27. Overall JE, Gorham DR (1962): The Brief Psychiatric Rating Scale. *Psychol Rep* 10: 799–812.
28. Andreasen NC (1982): Negative Symptoms in Schizophrenia: Definition and Reliability. *Arch Gen Psychiatry* 39: 784.
29. Buchanan RW, Javitt DC, Marder SR, Schooler NR, Gold JM, McMahon RP, *et al.* (2007): The Cognitive and Negative Symptoms in Schizophrenia Trial (CONSIST): The Efficacy of Glutamatergic Agents for Negative Symptoms and Cognitive Impairments. *Am J Psychiatry* 164: 1593–1602.
30. Birchwood M, Smith J, Cochrane R, Wetton S, Copestake S (1990): The Social Functioning Scale the Development and Validation of a New Scale of Social Adjustment for use in Family Intervention Programmes with Schizophrenic Patients. *Br J Psychiatry* 157: 853–859.
31. Heinrichs DW, Hanlon TE, Carpenter WT (1984): The Quality of Life Scale: An Instrument for Rating the Schizophrenic Deficit Syndrome. *Schizophr Bull* 10: 388–398.
32. Oliver LD, Haltigan JD, Gold JM, Foussias G, DeRosse P, Buchanan RW, *et al.* (2019): Lower- and Higher-Level Social Cognitive Factors Across Individuals With Schizophrenia Spectrum Disorders and Healthy Controls: Relationship With Neurocognition and Functional Outcome. *Schizophr Bull* 45: 629–638.
33. Nuechterlein KH, Green MF, Kern RS, Baade LE, Barch DM, Cohen JD, *et al.* (2008): The MATRICS Consensus Cognitive Battery, Part 1: Test Selection, Reliability, and Validity. *Am J Psychiatry* 165: 203–213.
34. Kohler CG, Bilker W, Hagendoorn M, Gur RE, Gur RC (2000): Emotion recognition deficit in schizophrenia: association with symptomatology and cognition. *Biol Psychiatry* 48: 127–136.
35. Baron-Cohen S, Wheelwright S, Hill J, Raste Y, Plumb I (2001): The "Reading the Mind in the Eyes" Test Revised Version: A Study with Normal Adults, and Adults with Asperger Syndrome or High-functioning Autism. *J Child Psychol Psychiatry* 42: 241–251.
36. McDonald S, Flanagan S, Rollins J (2011): The awareness of social inference test (revised). *New South Wales Aust Australas Soc Study Brain Impair*.
37. Esteban O, Markiewicz CJ, Blair RW, Moodie CA, Isik AI, Erramuzpe A, *et al.* (2019): fMRIPrep: a robust preprocessing pipeline for functional MRI. *Nat Methods* 16: 111–116.
38. Dickie EW, Anticevic A, Smith DE, Coalson TS, Manogaran M, Calarco N, *et al.* (2019): Ciftify: A framework for surface-based analysis of legacy MR acquisitions. *NeuroImage* 197: 818–826.
39. Glasser MF, Coalson TS, Robinson EC, Hacker CD, Harwell J, Yacoub E, *et al.* (2016): A multi-modal parcellation of human cerebral cortex. *Nature* 536: 171–178.

40. Tian Y, Margulies DS, Breakspear M, Zalesky A (2020): Topographic organization of the human subcortex unveiled with functional connectivity gradients. *Nat Neurosci* 23: 1421–1432.
41. Ji JL, Spronk M, Kulkarni K, Repovš G, Anticevic A, Cole MW (2019): Mapping the human brain's cortical-subcortical functional network organization. *NeuroImage* 185: 35–57.
42. Fortin J-P, Cullen N, Sheline YI, Taylor WD, Aselcioglu I, Cook PA, *et al.* (2018): Harmonization of cortical thickness measurements across scanners and sites. *NeuroImage* 167: 104–120.
43. Johnson WE, Li C, Rabinovic A (2007): Adjusting batch effects in microarray expression data using empirical Bayes methods. *Biostatistics* 8: 118–127.
44. Coifman RR, Lafon S, Lee AB, Maggioni M, Nadler B, Warner F, Zucker SW (2005): Geometric diffusions as a tool for harmonic analysis and structure definition of data: Diffusion maps. *Proc Natl Acad Sci* 102: 7426–7431.
45. Vos De Wael R, Benkarim O, Paquola C, Lariviere S, Royer J, Tavakol S, *et al.* (2020): BrainSpace: a toolbox for the analysis of macroscale gradients in neuroimaging and connectomics datasets. *Commun Biol* 3: 103.
46. Krishnan A, Williams LJ, McIntosh AR, Abdi H (2011): Partial Least Squares (PLS) methods for neuroimaging: a tutorial and review. *Neuroimage* 56: 455–475.
47. Berry KJ, Johnston JE, Mielke PW (2011): Permutation methods. *WIREs Comput Stat* 3: 527–542.
48. Hesterberg T (2011): Bootstrap. *WIREs Comput Stat* 3: 497–526.
49. R Development Core Team (2010): R: A language and environment for statistical computing. Vienna, Austria: R Foundation for Statistical Computing. Retrieved from http://www.R-project.org
50. Hanlon FM, Shaff NA, Dodd AB, Ling JM, Bustillo JR, Abbott CC, *et al.* (2016): Hemodynamic response function abnormalities in schizophrenia during a multisensory detection task: Hemodynamic Response Function Abnormalities. *Hum Brain Mapp* 37: 745–755.
51. Gröhn C, Norgren E, Eriksson L (2022): A systematic review of the neural correlates of multisensory integration in schizophrenia. *Schizophr Res Cogn* 27: 100219.
52. Anticevic A, Cole MW, Repovs G, Murray JD, Brumbaugh MS, Winkler AM, *et al.* (2014): Characterizing Thalamo-Cortical Disturbances in Schizophrenia and Bipolar Illness. *Cereb Cortex* 24: 3116–3130.
53. Damaraju E, Allen EA, Belger A, Ford JM, McEwen S, Mathalon DH, *et al.* (2014): Dynamic functional connectivity analysis reveals transient states of dysconnectivity in schizophrenia. *NeuroImage Clin* 5: 298–308.
54. Woodward ND, Karbasforoushan H, Heckers S (2012): Thalamocortical Dysconnectivity in Schizophrenia. *Am J Psychiatry* 169: 1092–1099.
55. Andreasen NC, Paradiso S, O'Leary DS (1998): "Cognitive Dysmetria" as an Integrative Theory of Schizophrenia: A Dysfunction in Cortical-Subcortical-Cerebellar Circuitry? *Schizophr Bull* 24: 203–218.
56. Bethlehem RAI, Paquola C, Seidlitz J, Ronan L, Bernhardt B, Consortium C-C, Tsvetanov KA (2020): Dispersion of functional gradients across the adult lifespan. *NeuroImage* 222: 117299.
57. Cross N, Paquola C, Pomares FB, Perrault AA, Jegou A, Nguyen A, *et al.* (2021): Cortical gradients of functional connectivity are robust to state-dependent changes following sleep deprivation. *NeuroImage* 226: 117547.
58. Girn M, Roseman L, Bernhardt B, Smallwood J, Carhart-Harris R, Nathan Spreng R (2022): Serotonergic psychedelic drugs LSD and psilocybin reduce the hierarchical differentiation of unimodal and transmodal cortex. *NeuroImage* 256: 119220.
59. Xia M, Liu J, Mechelli A, Sun X, Ma Q, Wang X, *et al.* (2022): Connectome gradient dysfunction in major depression and its association with gene expression profiles and treatment outcomes. *Mol Psychiatry*. https://doi.org/10.1038/s41380-022-01519-5
60. Choi H, Byeon K, Park B, Lee J, Valk SL, Bernhardt B, *et al.* (2022): Diagnosis-informed connectivity subtyping discovers subgroups of autism with reproducible symptom profiles. *NeuroImage* 256: 119212.

61. Huntenburg JM, Bazin P-L, Goulas A, Tardif CL, Villringer A, Margulies DS (2017): A Systematic Relationship Between Functional Connectivity and Intracortical Myelin in the Human Cerebral Cortex. *Cereb Cortex* 27: 981–997.
62. Huntenburg JM, Bazin P-L, Margulies DS (2018): Large-Scale Gradients in Human Cortical Organization. *Trends Cogn Sci* 22: 21–31.
63. Blazquez Freches G, Haak KV, Bryant KL, Schurz M, Beckmann CF, Mars RB (2020): Principles of temporal association cortex organisation as revealed by connectivity gradients. *Brain Struct Funct* 225: 1245–1260.
64. Burt JB, Demirtaş M, Eckner WJ, Navejar NM, Ji JL, Martin WJ, *et al.* (2018): Hierarchy of transcriptomic specialization across human cortex captured by structural neuroimaging topography. *Nat Neurosci* 21: 1251–1259.
65. Flynn SW, Lang DJ, Mackay AL, Goghari V, Vavasour IM, Whittall KP, *et al.* (2003): Abnormalities of myelination in schizophrenia detected in vivo with MRI, and post-mortem with analysis of oligodendrocyte proteins. *Mol Psychiatry* 8: 811–820.
66. Vanes LD, Mouchlianitis E, Barry E, Patel K, Wong K, Shergill SS (2019): Cognitive correlates of abnormal myelination in psychosis. *Sci Rep* 9: 5162.
67. Voineskos AN, Mulsant BH, Dickie EW, Neufeld NH, Rothschild AJ, Whyte EM, *et al.* (2020): Effects of Antipsychotic Medication on Brain Structure in Patients With Major Depressive Disorder and Psychotic Features: Neuroimaging Findings in the Context of a Randomized Placebo-Controlled Clinical Trial. *JAMA Psychiatry* 77: 674.
68. Sarpal DK, Argyelan M, Robinson DG, Szeszko PR, Karlsgodt KH, John M, *et al.* (2016): Baseline Striatal Functional Connectivity as a Predictor of Response to Antipsychotic Drug Treatment. *Am J Psychiatry* 173: 69–77.

Figure/Table Legends

Figure 1. Principal gradient analysis and partial least squares correlation (PLSC). A illustrates the Glasser atlas, with 360 regions categorized into 12 networks from the Cole-Anticevic Brain Network Parcellation, indicated by different colors. **B** and **C** illustrate the network segregations of the three gradients respectively in brain and in the gradient space. **B** shows the average gradient scores across all participants (purple for positive scores and yellow for negative scores). **C** shows the average gradient scores across all participants in two scatter plots, respectively for Gradients 1 vs. 2 and for Gradient 2 vs. 3. In these scatter plots, each small dot represents a brain region and is colored according to its network; the bigger opaque dots illustrate the mean gradient scores of all 12 networks. Overall, Gradient 1 features Somatosensory vs. Frontoparietal network segregation; Gradient 2 features Auditory/Motor vs. Visual network segregation; and Gradient 3 features Default mode vs. Frontoparietal network segregation. **D** illustrates the PLSC procedure (see more details in **Supplementary Materials**).

Figure 2. Group differences in Gradients 1-3. A shows the brain regions with significant group differences according to two-sample *t*-tests (as linear models). Warm colors indicate SSDs being significantly closer to, respectively for each gradient, the frontoparietal, the vision, or the frontoparietal networks than Controls; cold colors indicate SSDs being significantly closer to, respectively for each gradient, the somatosensory, the auditory/motor, or the default mode networks than Controls. **B**–**D** show the brain regions with group differences along Gradients 1–3 in a 3D space; specifically, **C** shows the regions with a significant group difference along Gradient 2 (i.e., the x-axis of the plot), and **D** shows the regions with a significant group difference along Gradient 3 (i.e., the y-axis of the plot). These three figures show how each ROI moves along the three gradients from Controls to SSD (as indicated by the arrows). Each arrow represents one ROI and is colored according to the networks defined by Cole-Anticevic (cortical) and Tian (subcortical) parcellations in **Figure 1A**. The network labels illustrate where the means of the networks are for Controls.

Figure 3. **The first dimension of PLSC.** The loadings for the cognitive measures (**A**) and the network hierarchy (**B**) illustrate the general associations of the cognitive measures and the network hierarchy. The latent variables of Dimension 1 are shown in **C** where SSDs and Controls are significantly different according to bootstrap tests both according to the network hierarchy and to their cognitive measures. Together, **A** and **B** show associations that contribute to the group differences shown in **C**. Because this dimension is characterized by the group difference, in **D**-**F**, we highlighted such group differences (indicated by the arrows) of the identified regions of interest (ROIs) on Gradients 1 (**D**), 2 (**E**), and 3 (**F**). The highlighted arrows in these figures illustrate the group differences in the identified ROI gradients that most relate to cognition according to PLSC. On these figures, each arrow indicates the change from Controls to SSDs. The opaqueness of the arrows illustrates the amount of scaled contributions (i.e., squared loadings × 100), and the shape of the starting point illustrates the direction of how these ROIs load on Dimension 1 of PLSC (i.e., positive as square and negative as circle). The network labels illustrate where the means of the networks are for Controls.

Figure 4. Correlations between cognitive and brain scores and clinical and functioning outcomes. A shows the scatter plot between the latent variable pair and the total scores of the clinical and functioning measures with correlation lines illustrating the linear relationships. Blue lines indicate significantly negative correlations and red lines indicate significantly positive correlations. **B** shows the squared correlation between the latent variable pair, brain scores (colored in purple) and cognitive scores (colored in dark green), and the subscales in the Birchwood Social Functioning Scale (BSFS; colored in black), the Quality of Life Scale (QLS; colored in pink), the Brief Psychiatric Rating Scale (BPRS; colored in green), and the Scale of the Assessment of Negative Symptoms (SANS; colored in cyan). The blue circles indicate positive correlations, and the red circles indicate negative correlations. The shaded area marks the magnitude of squared coefficients of correlation that are not significant in the Pearson correlation test.

Table 1. Demographics and Behavioral Characteristics. The table shows the means and standard deviations (SD) of the demographics and the clinical and behavioral characteristics of each participant group. The statistics of examining the group effects are shown in the last three columns for each variable.

Table 2. Significant group differences in regions of interest (ROIs) on Gradients 1-3. The table summarizes the group effects found in all three gradients by networks and lists, for each network, the range of the significant *F* statistics and the number of significant ROIs.

Table 3. Correlation between latent variables and clinical and functioning subscales. The table shows how cognitive scores and brain scores correlate with the individual subscales of the Birchwood Social Functioning Scale (BSFS), the Quality of Life Scale (QLS), and two scales of symptoms, the Brief Psychiatric Rating Scale (BPRS) and the Scale of the Assessment of Negative Symptoms (SANS). The coefficients of correlation are reported along with their 95% confidence intervals (CI), and *q*(FDR) shows the FDR-corrected *p*-value for all 38 correlation tests. In these correlation tests, QLS intrapsychic foundations, QLS common objects and activities, and SANS avolition/apathy have 1 missing value. SANS asociality/anhedonia have 2 missing values.

Tables

Table 1. Demographics and Behavioral Characteristics.

	SSD (n = 248)	Control (n = 172)			
	Mean (SD)	Mean (SD)	*df**	*t*	*q*(FDR)
Age (years)	31.42 (9.77)	31.95 (10.40)	352.94	-0.53‡	.597
Female (*n*; %)	79 (31.85%)	80 (46.51%)			
Mean framewise displacement (FD; mm)	0.16 (0.1)	0.14 (0.08)	415	1.51	.139
Parental education level – Father (years)	14.48 (3.18)	15.40 (3.07)	186.55	-2.12‡	.035
Parental education level – Mother (years)	14.08 (3.06)	14.93 (2.63)	198.03	-2.16‡	.032
Wechsler Test of Adult Reading (WTAR) Standard Score	108.11 (14.31)	113.71 (10.81)	167	-2.67	< .001
Chlorpromazine (CPZ) equivalents	463.68 (382.37)	--	--	--	--
Clinical measures					
Brief Psychiatric Rating Scale (BPRS)	31.35 (7.86)	--	--	--	--
Scale for the Assessment of Negative Symptoms (SANS)	25.12 (12.31)	--	--	--	--
Birchwood Social Functioning Scale (BSFS)	136.34 (23.16)	175.16 (19.21)	--	--	< .001§
Quality of Life Scale (QLS)	73.66 (20.96)	--	--	--	--
Social cognitive measures					
Penn Emotion Recognition Task (ER40)	31.84 (4.55)	33.55 (3.32)	413	-4.2	< .001
Reading the Mind in the Eyes Test (RMET)	24.57 (5.26)	27.60 (3.82)	417	-6.45	< .001
TASIT 1	22.50 (3.64)	24.64 (2.14)	418	-6.92	< .001
TASIT 2 paradoxical sarcasm	15.73 (3.95)	18.52 (2.09)	418	-8.48	< .001
TASIT 2 simple sarcasm	14.89 (4.94)	18.47 (1.92)	418	-9.06	< .001
TASIT 2 sincere	16.92 (3.19)	17.48 (2.69)	418	-1.91	.061
TASIT 3 lies	24.82 (4.12)	27.25 (3.64)	393.52	-6.34‡	< .001
TASIT 3 sarcasm	23.53 (5.15)	27.47 (3.62)	415	-8.65	< .001
Non-social cognitive measures (MCCB)					
Processing speed	39.69† (13.16)	53.06† (10.10)	--	--	< .001§
Reasoning and problem solving	42.91 (10.97)	48.76 (9.54)	397.13	-5.8‡	< .001
Attention/Vigilance	39.50 (11.66)	47.65 (12.72)	345.66	-6.64‡	< .001
Working memory	41.27† (11.19)	49.16 (11.36)	--	--	< .001§
Verbal learning	40.67 (8.94)	50.30 (9.44)	354.82	-10.51‡	< .001
Visual learning	38.73 (12.46)	48.38 (10.06)	418	-8.43	< .001

† denotes a sample that did not pass the normality test, ‡ denotes a Welch's *t*, and § denotes results from a bootstrap test. * The degrees of freedom change between measures because of the tests being used (i.e., a *t*-test, a Welch's *t*-test, or a bootstrap *t* test) and the number of missing values before the imputation.

Table 2. Significant group differences in regions of interest (ROIs) on Gradients 1-3.

	Gradient 1		Gradient 2		Gradient 3	
Networks	*F* range	*n* of ROIs	*F* range	*n* of ROIs	*F* range	*n* of ROIs
Visual1	[-4.79, -3.52]	4	[2.65, 2.93]	2	[-5.04, -5.02]	2
Visual2	[-5.07, -2.96]	9	[2.59, 5.6]	41	[-3.97, 5.65]	14
Somatomotor	[-3.58, -2.62]	13	[-6.27, -2.69]	21	[-2.91, 3.12]	2
Cingulo-Opercular	[2.61, 3.42]	12	[-6.72, -2.59]	32	[2.75, 3.32]	5
Dorsal-Attention	[-3.11, -2.57]	3	[2.83, 4.89]	9	[-4.38, -2.64]	4
Language	[3.7, 3.7]	1	[-2.64, -2.64]	1	[-4, -2.79]	7
Frontoparietal	[2.76, 4.09]	4	[-4.03, -3.73]	3	--	0
Auditory	[2.75, 3.08]	6	[-5.56, -2.82]	12	[-3, -3]	1
Default	[-5.59, -2.62]	8	[-4.34, 4.43]	11	[2.62, 3.24]	2
Posterior-Multimodal	--	0	--	0	[-2.91, -2.91]	1
Ventral-multimodal	--	0	--	0	--	0
Orbito-Affective	--	0	[-2.72, -2.72]	1	--	0
Subcortical	[2.83, 4.76]	6	[-4.83, -2.6]	4	[2.64, 4.57]	11

Table 3. Correlation between latent variables and clinical and functioning subscales.

	Correlation with Cognitive Scores		Correlation with Brain Scores	
	r [95% CI]	*q*(FDR)	*r* [95% CI]	*q*(FDR)
Birchwood Social Functioning Scale (BSFS)				
Social engagement/withdrawn	.02 [-.11, .14]	.823	-.02 [-.15, .1]	.785
Interpersonal communication/relationship	-.05 [-.17, .07]	.490	-.10 [-.22, .03]	.174
Interpersonal prosocial activity subscale	-.08 [-.20, .05]	.284	-.15 [-.27, -.03]	.031
Recreation activity	-.21 [-.32, -.08]	.004	-.24 [-.36, -.12]	.001
Independence performance	-.14 [-.26, -.02]	.044	-.15 [-.27, -.02]	.036
Independence competence	-.23 [-.34, -.11]	.001	-.10 [-.22, .03]	.175
Quality of Life Scale (QLS)				
Interpersonal behavior	-.25 [-.36, -.13]	.001	-.20 [-.32, -.08]	.004
Instrumental role	-.27 [-.38, -.15]	< .001	-.24 [-.35, -.12]	.001
Intrapsychic foundations	-.28 [-.39, -.16]	< .001	-.23 [-.34, -.1]	.001
Common objects and activities	-.32 [-.43, -.21]	< .001	-.28 [-.39, -.16]	< .001
Brief Psychiatric Rating Scale (BPRS)				
Negative symptoms	.15 [.03, .27]	.032	.09 [-.04, .21]	.235
Positive symptoms	.18 [.05, .30]	.012	.07 [-.06, .19]	.348
Anxiety/depression	-.06 [-.18, .07]	.436	.10 [-.02, .22]	.170
Activation	0 [-.13, .12]	.970	.01 [-.12, .13]	.935
Hostility	.12 [-.01, .24]	.101	.02 [-.1, .15]	.790
Scale for the Assessment of Negative Symptoms (SANS)				
Affective flattening or blunting	.15 [.03, .27]	.031	.14 [.02, .26]	.044
Alogia	.33 [.21, .43]	< .001	.21 [.09, .32]	.003
Avolition/apathy	.16 [.03, .28]	.031	.19 [.07, .31]	.006
Asociality/anhedonia	.12 [-.01, .24]	.099	.19 [.07, .31]	.006

QLS intrapsychic foundations, QLS common objects and activities, and SANS avolition/apathy have 1 missing value. SANS asociality/anhedonia have 2 missing values.

Figure1

A

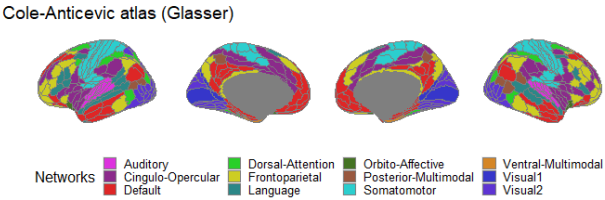

B

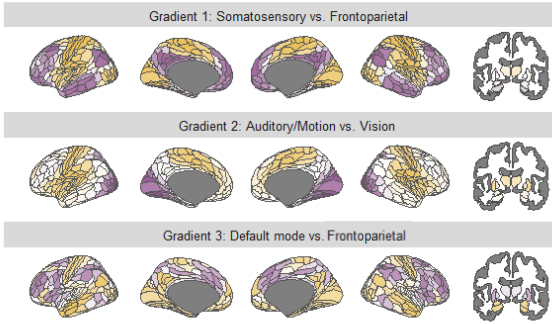

C

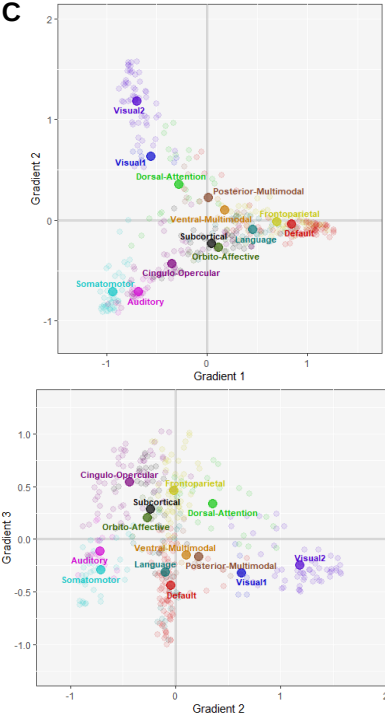

D

Social cognitive measures

- **Reading the Mind in the Eyes Test (RMET)**
  Mental state inference from static eye region of faces
- **Penn Emotion Recognition Test (ER40)**
  Basic emotion recognition from static faces
- **The Awareness of Social Inference Test-Revised (TASIT)**
  - **TASIT 1: Emotion Evaluation Task**
    Basic emotion recognition from videos
  - **TASIT 2: Social Inference (Minimal)**
    Sincere, simple sarcastic, and paradoxical sarcastic exchanges
  - **TASIT 3: Social Inference (Enriched)**
    Lies and sarcastic exchanges, with enriched contextual cues

Non-social (neuropsychological) cognitive measures

- **MATRICS Consensus Cognitive Battery (MCCB) Domain scores:**

Processing speed	Verbal Learning
Attention/Vigilance	Visual Learning
Working Memory	Reasoning and Problem Solving

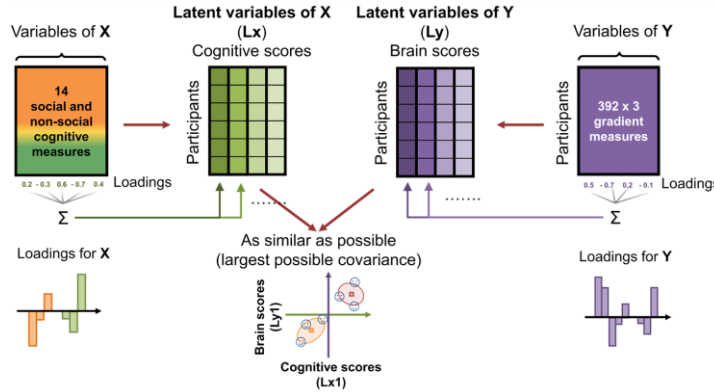

Figure2

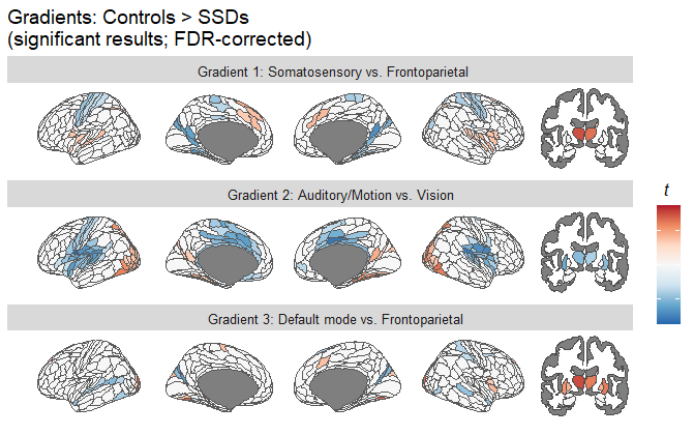
A
Gradients: Controls > SSDs
(significant results; FDR-corrected)
Gradient 1: Somatosensory vs. Frontoparietal
Gradient 2: Auditory/Motion vs. Vision
Gradient 3: Default mode vs. Frontoparietal
t
4
0
-4

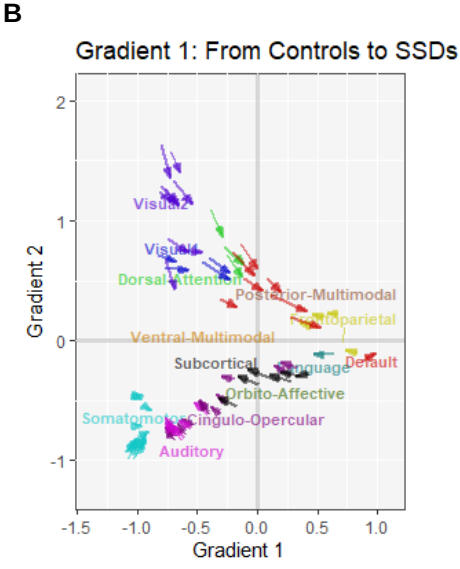
B
Gradient 1: From Controls to SSDs
Gradient 1
Gradient 2
Visual2
Visual1
Dorsal-Attention
Posterior-Multimodal
Frontoparietal
Ventral-Multimodal
Subcortical
Language
Default
Orbito-Affective
Somatomotor
Cingulo-Opercular
Auditory

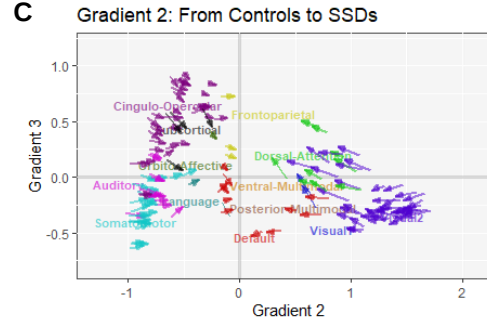
C
Gradient 2: From Controls to SSDs
Gradient 2
Gradient 3
Cingulo-Opercular
Frontoparietal
Subcortical
Dorsal-Attention
Orbito-Affective
Auditory
Ventral-Multimodal
Language
Posterior-Multimodal
Somatomotor
Default
Visual1
Visual2

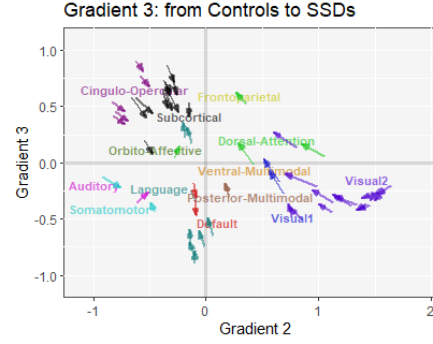
D
Gradient 3: from Controls to SSDs
Gradient 2
Gradient 3
Cingulo-Opercular
Frontoparietal
Subcortical
Dorsal-Attention
Orbito-Affective
Ventral-Multimodal
Auditory
Language
Visual2
Posterior-Multimodal
Somatomotor
Visual1
Default

Figure

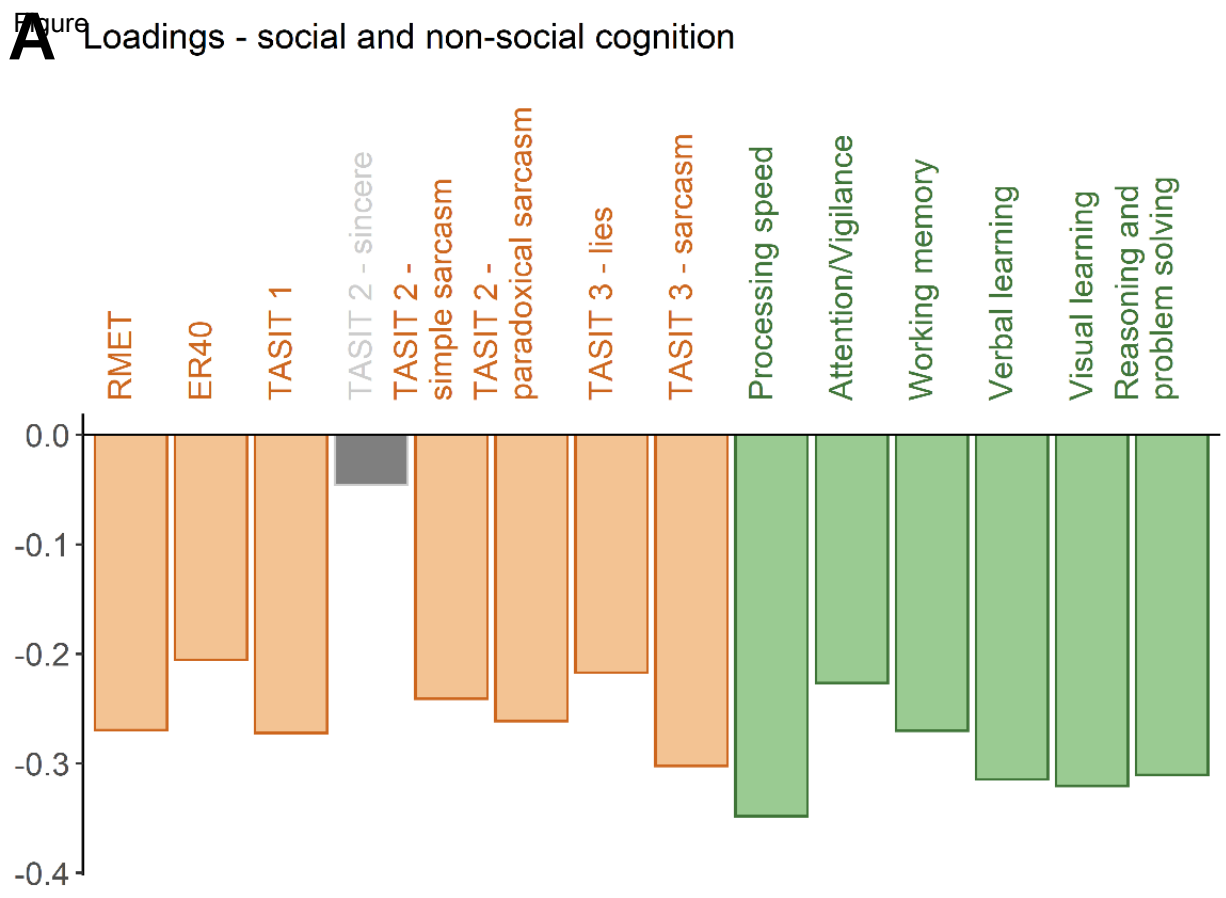
A
Loadings - social and non-social cognition
RMET
ER40
TASIT 1
TASIT 2 - sincere
TASIT 2 - simple sarcasm
TASIT 2 - paradoxical sarcasm
TASIT 3 - lies
TASIT 3 - sarcasm
Processing speed
Attention/Vigilance
Working memory
Verbal learning
Visual learning
Reasoning and problem solving
0.0
-0.1
-0.2
-0.3
-0.4

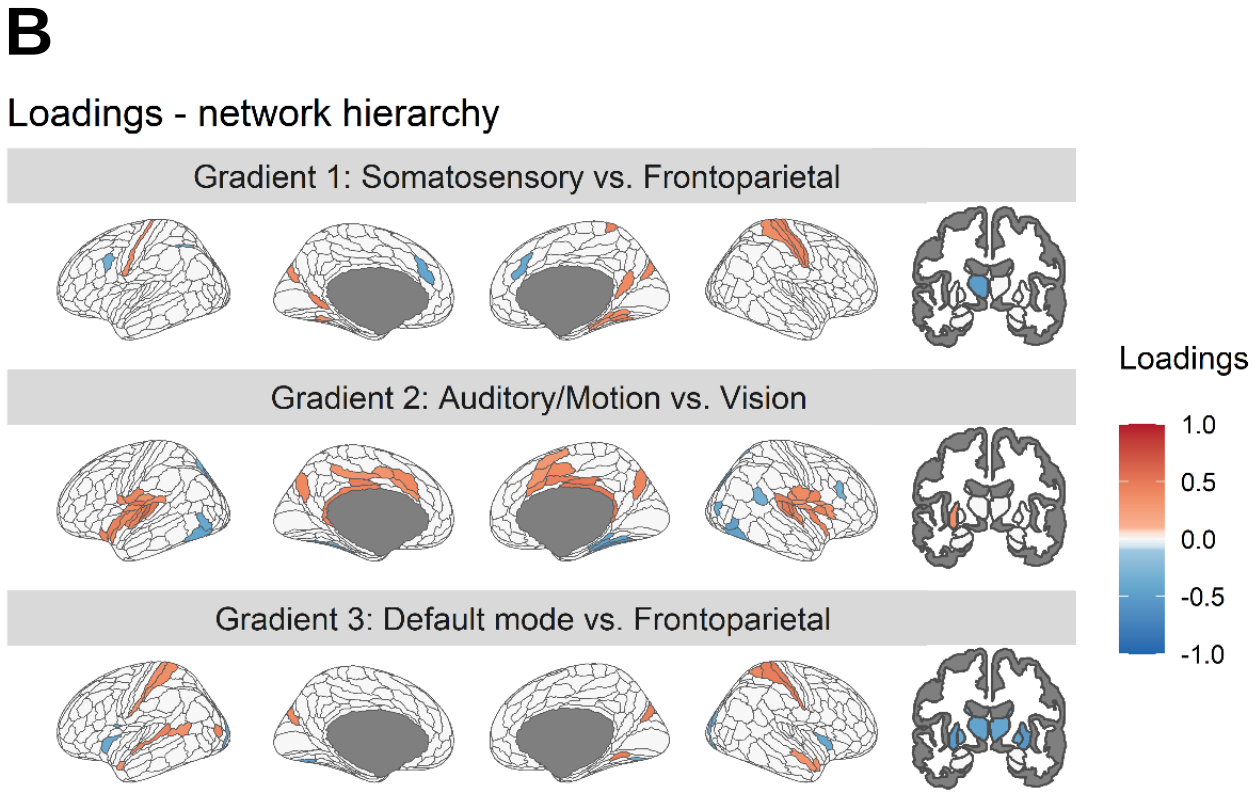
B
Loadings - network hierarchy
Gradient 1: Somatosensory vs. Frontoparietal
Gradient 2: Auditory/Motion vs. Vision
Gradient 3: Default mode vs. Frontoparietal
Loadings
1.0
0.5
0.0
-0.5
-1.0

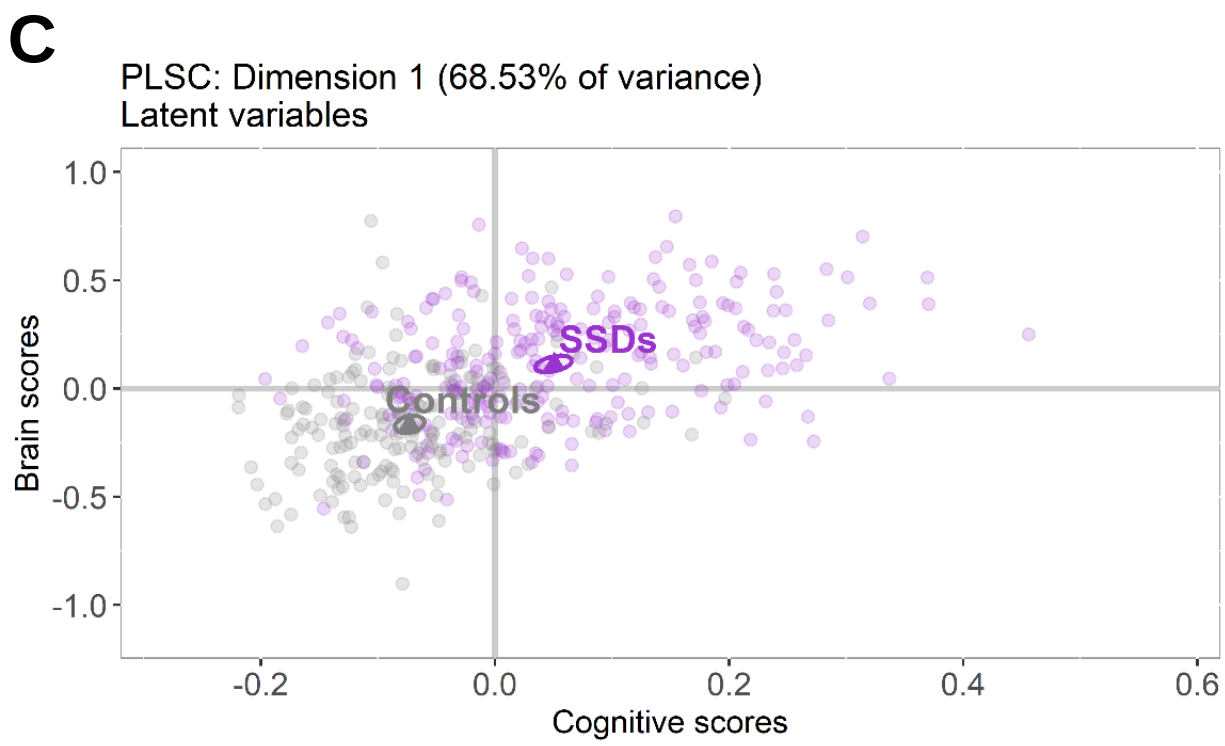
C
PLSC: Dimension 1 (68.53% of variance)
Latent variables
SSDs
Controls
Brain scores
Cognitive scores
1.0
0.5
0.0
-0.5
-1.0
-0.2
0.0
0.2
0.4
0.6

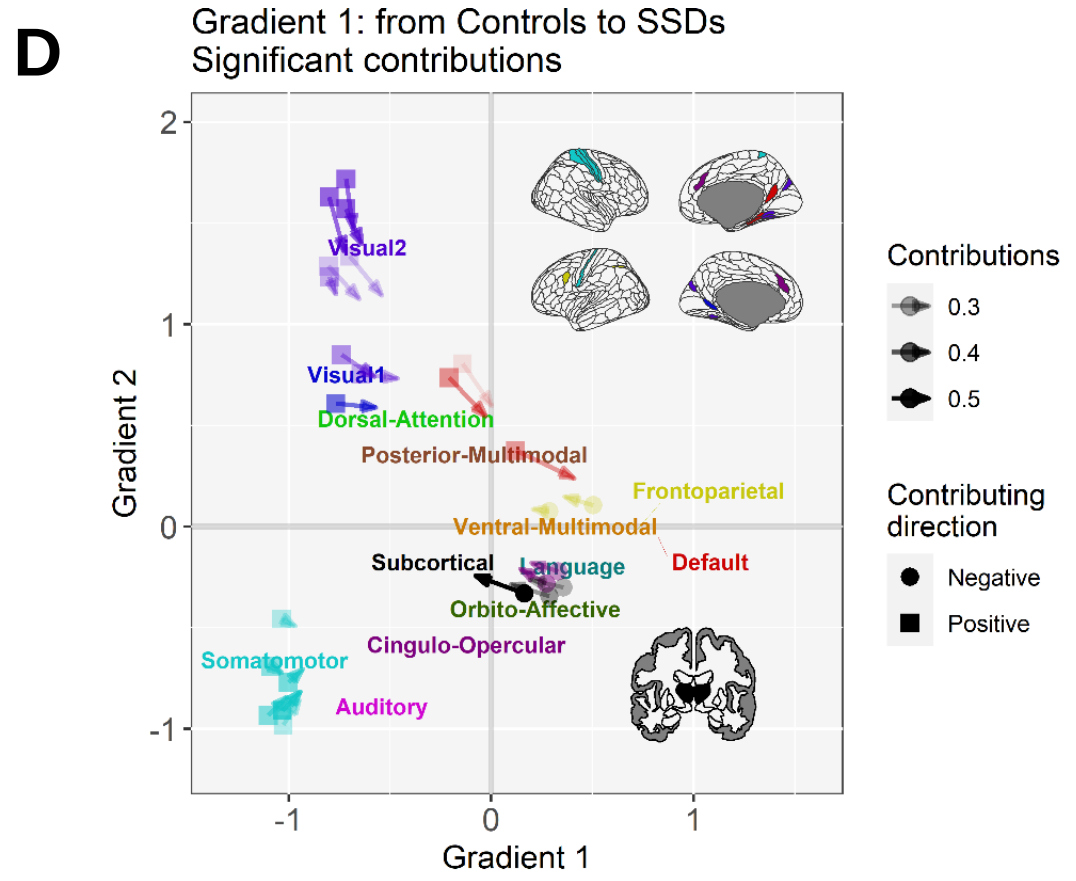
D
Gradient 1: from Controls to SSDs
Significant contributions
Visual2
Visual1
Dorsal-Attention
Posterior-Multimodal
Frontoparietal
Ventral-Multimodal
Subcortical
Language
Default
Orbito-Affective
Somatomotor
Cingulo-Opercular
Auditory
Gradient 2
Gradient 1
Contributions
0.3
0.4
0.5
Contributing direction
Negative
Positive

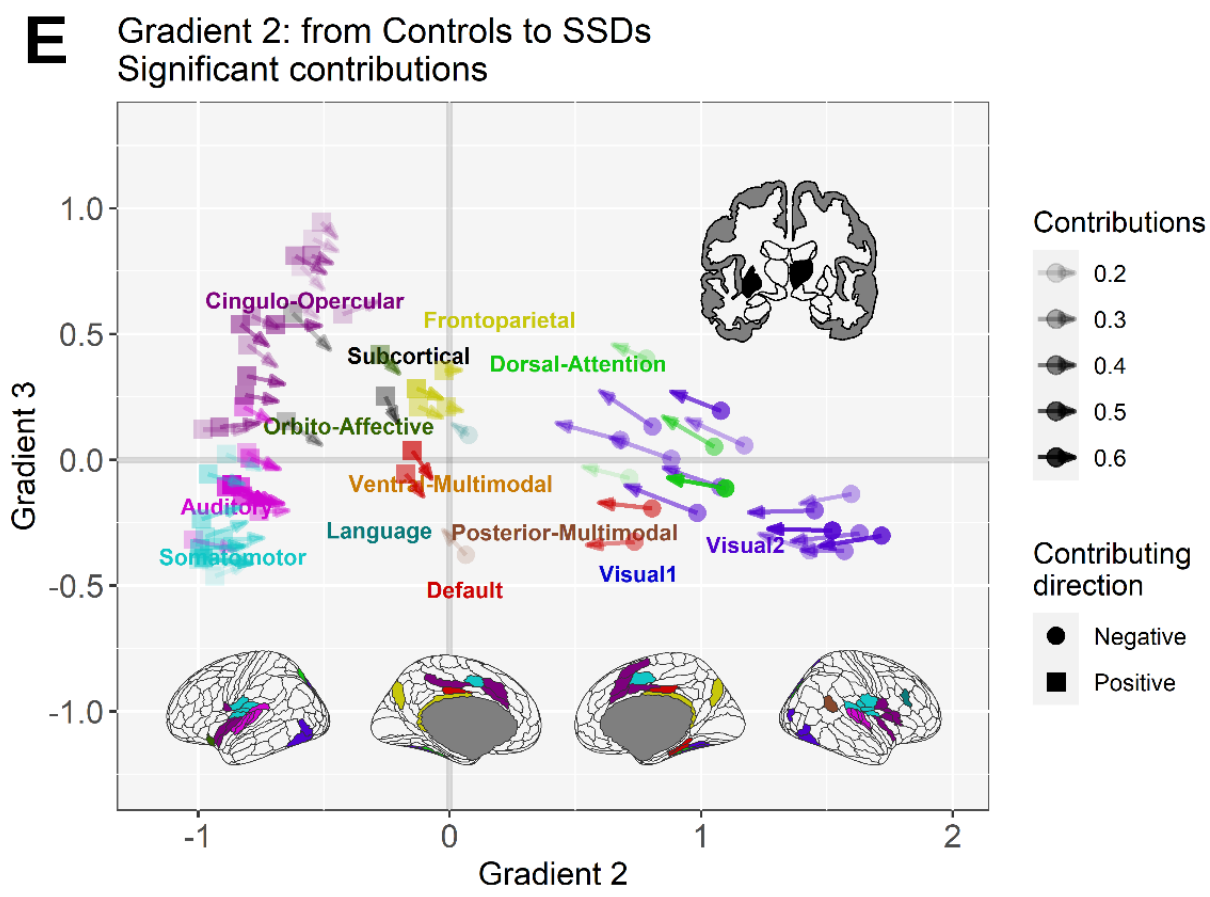
E
Gradient 2: from Controls to SSDs
Significant contributions
Cingulo-Opercular
Frontoparietal
Subcortical
Dorsal-Attention
Orbito-Affective
Ventral-Multimodal
Auditory
Language
Posterior-Multimodal
Visual2
Somatomotor
Visual1
Default
Gradient 3
Gradient 2
Contributions
0.2
0.3
0.4
0.5
0.6
Contributing direction
Negative
Positive

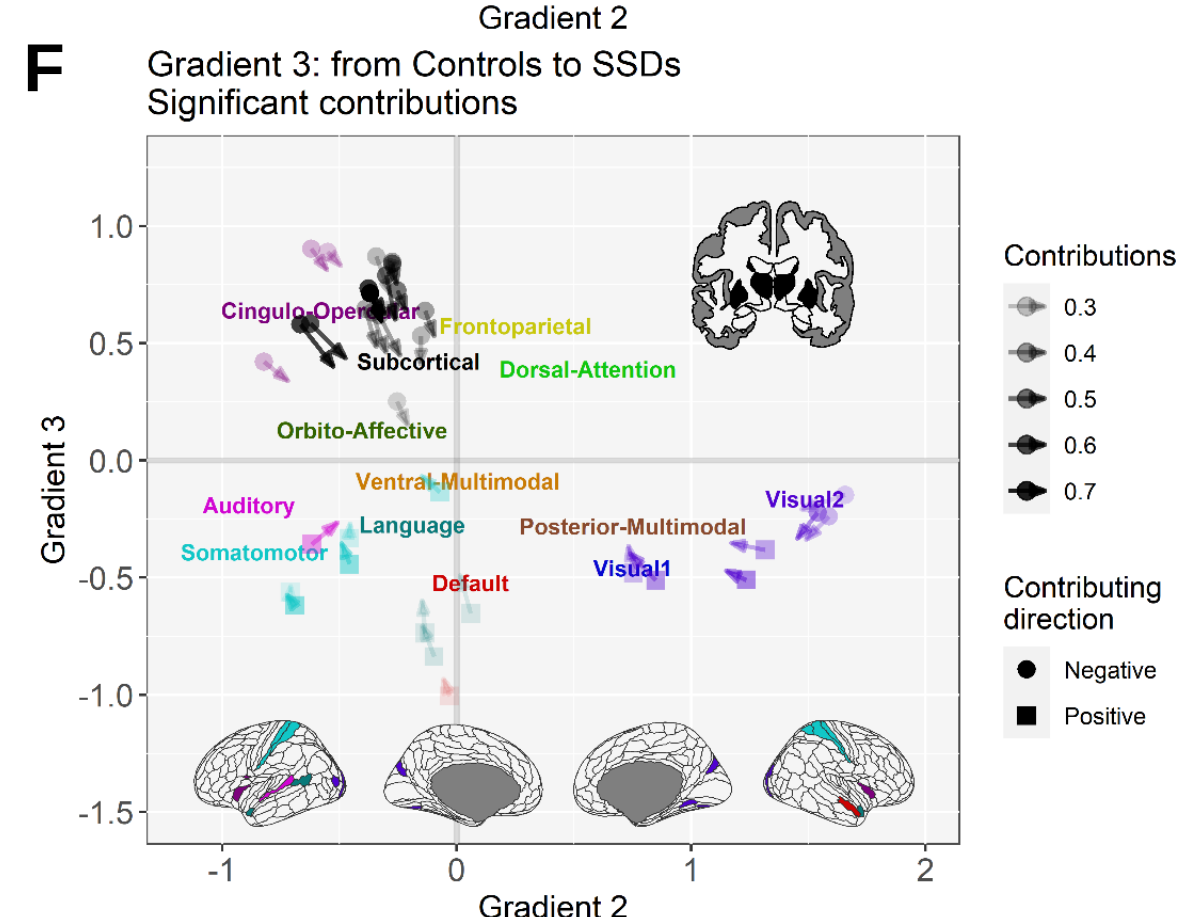
F
Gradient 3: from Controls to SSDs
Significant contributions
Cingulo-Opercular
Frontoparietal
Subcortical
Dorsal-Attention
Orbito-Affective
Ventral-Multimodal
Auditory
Language
Posterior-Multimodal
Visual2
Somatomotor
Visual1
Default
Gradient 3
Gradient 2
Contributions
0.3
0.4
0.5
0.6
0.7
Contributing direction
Negative
Positive

Figure4

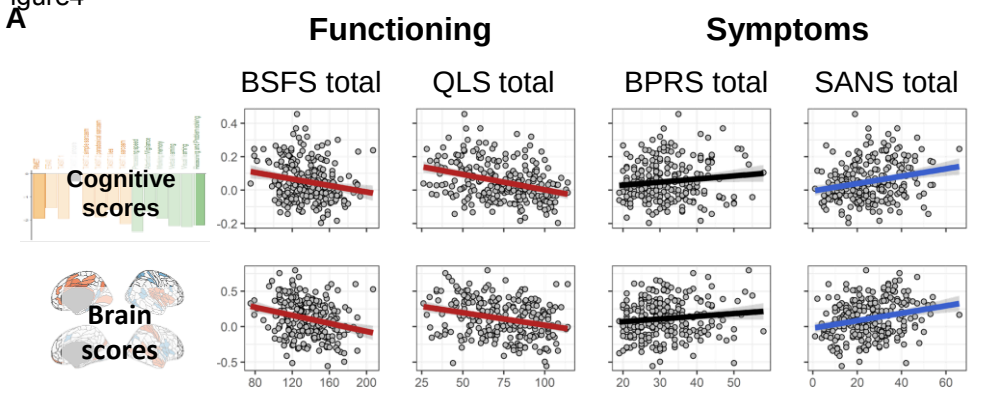
A
Functioning
Symptoms
BSFS total
QLS total
BPRS total
SANS total
Cognitive scores
Brain scores

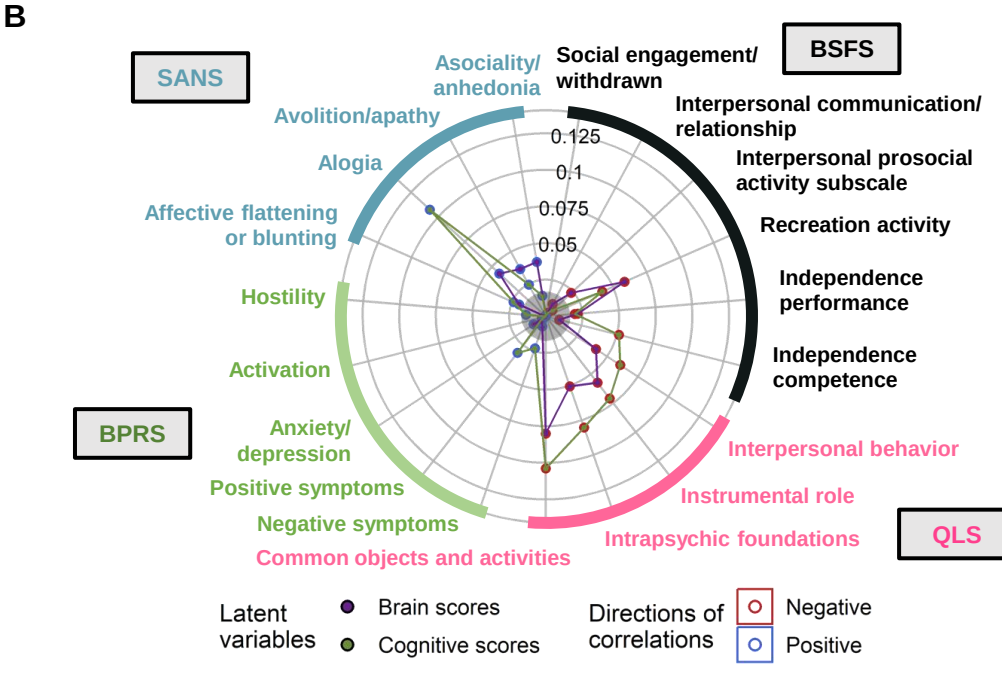
B
SANS
BSFS
BPRS
QLS
Asociality/ anhedonia
Social engagement/ withdrawn
Avolition/apathy
Interpersonal communication/ relationship
Alogia
Interpersonal prosocial activity subscale
Affective flattening or blunting
Recreation activity
Hostility
Independence performance
Activation
Independence competence
Anxiety/ depression
Interpersonal behavior
Positive symptoms
Instrumental role
Negative symptoms
Intrapsychic foundations
Common objects and activities
0.125
0.1
0.075
0.05
Latent variables
Brain scores
Cognitive scores
Directions of correlations
Negative
Positive

Supplement (Word doc) Click here to access/download;Supplement (Word doc);Ju-Chi_Supp_Gradients PLSC 2024_BioPsych.docx

Supplementary materials

Methods

Participants

The following figure illustrates the inclusion/exclusion criteria at each stage of data analysis.

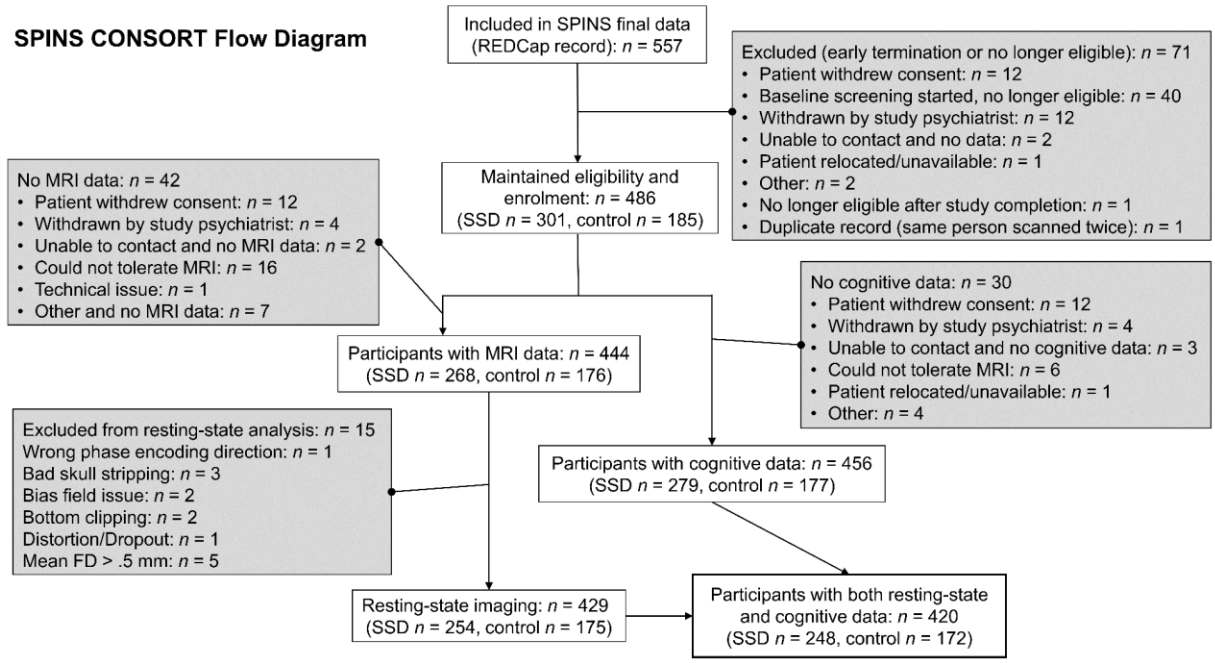

Figure S1. The data from SPINS recruited 557 participants with 486 eligible participants (301 for SSD and 185 for controls). We excluded data for statistical analysis based on quality control (QC) criteria that include screenings of the structural image (i.e., Dashboard QC), the functional magnetic resonance imaging (fMRI) preprocessing outputs (i.e., fMRIPrep/Ciftify QC), and excessive motion captured by framewise displacement (FD). The final sample includes 248 participants with SSDs and 172 healthy controls who have both complete cognitive and resting-state fMRI data.

MRI Data Acquisition

MRI data was collected across 6 scanners, including a General Electric Discovery (*N* = 135) and Siemens Prisma (*N* = 30) at CAMH, a General Electric Signa (*N* = 42) and Siemens Prisma (*N* = 98) at ZHH, and a Siemens Tim Trio (*N* = 66) and Siemens Prisma (*N* = 79) at MPRC. To ensure sequence stability over time and minimize inter-site variance, standardized operating procedures were used along with weekly phantom scans. The study also provided objective evidence for inter-site stability (1–3) . Due to scanner differences there were slight variations in the parameters for the T1 MRIs: CMH and ZHH used a BRAVO sequence with TR=6.7/6.4 ms, TE=3/2.8 ms, flip angle=8°, field of view=230 mm, in plane resolution=0.9 mm^2, slice thickness=0.9 mm; CMP, MRC, MRP, and ZHP used an MPRAGE sequence with TR=2300 ms, TE=2.9 ms, flip angle=9°, field of view=230 mm, in plane resolution=0.9 mm^2, slice

thickness=0.9 mm).The Resting State (RS) scan was also part of a longer multimodal MRI protocol previously described (4).

MRI Preprocessing

The fMRI data were preprocessed using fMRIPrep 1.5.8 (5) and Nipype 1.4.1 (6). Anatomical T1-weighted images were corrected for intensity non-uniformity and skull-stripped using ANTs 2.2.0, and brain tissue segmentation was performed by FSL 5.0.9 (7). Brain surfaces were reconstructed using FreeSurfer 6.0.1 (8), For each fMRI run, ANTs (9) was used to perform fieldmap-less distortion correction, and the Freesurfer's boundary-based registration, with six degrees of freedom, was performed for co-registration of the functional data to the corresponding T1-weighted image. Slice-timing correction and motion correction were performed using MCFLIRT (FSL 5.0.9) (10).

Following fMRIPrep, the ciftify workflows (11) version 2.3.1 were used to convert the freesurfer reconstructed surfaces to gifti and cifti file formats. The cortical surfaces were realigned to the HCP fsLR templates (12), using sulcal depth using the MSM algorithm (MSMSulc) (13) and resampled to 32k vertices per hemisphere, and the freesurfer subcortical segmentation was used to define the participants 32k subcortical atlas greyordinates. The functional data was projected to the 32k surface coordinates using a ribbon constrained method that excludes outlier voxels, with methods similar to those employed by the HCP Pipelines (12).

We dropped the first three TRs for each scan, and performed spatial smoothing with a 2 mm full width at half maximum Gaussian kernel. 'ciftify_clean_img' was then used to detrend and band-pass filter (0.01-0.1 Hz) the signals and perform nuisance regression on the data. The nuisance regression model included six head motion correction parameters, mean white matter signal, mean cerebral spinal fluid signal, mean global signal and the square, the derivative, and the squared derivative for each of these regressors (generated by fMRIPrep). We regressed out the mean global signal to remove the dominating global effects.

Statistical Analysis

For any participants missing one cognitive measure, data were imputed with the rest of the behavioral variables using the *mice* package in R. To examine group differences in cognition, we first examined the homoscedasticity between groups by *F*-tests and confirmed the normality of each group by Shapiro-Wilk's test. Next, we examined group differences between SSDs and controls before imputing missing data. We performed the two-sample equal variances *t*-test if the measure showed homoscedasticity between groups, and we performed the Welch's unequal variances *t*-test if the groups are heteroscedastic. If either group did not pass the normality test, we performed a non-parametric bootstrap *t*-test, which has no normality assumption of the data.

Partial Least Squares Correlation (PLSC)

Partial least squares correlation (PLSC) (14) is a component-based method that is used to examine the association between two sets of variables measuring the same participants. PLSC decomposes the cross product between the two variable sets. In our analysis, with the variables centered and normalized to have sums of squares of 1s, such cross product gives scaled correlations between the two sets of variables. PLSC then decomposes such cross product matrix into uncorrelated *dimensions* that best capture different components of the correlation pattern. In

PLSC, each dimension is composed of 1) two sets of *latent variables*, which represent the participants on this dimension, with respect to the two sets of variables (i.e., behavioral and gradients), and 2) two sets of variable *loadings*, which describe how they contribute to this dimension.

Formally, latent variables are new variables obtained by linear combinations (weighted sums) of the original variables. Each dimension of PLSC includes one pair of latent variables—one obtained from each data table—and the coefficients used to compute these linear combinations are the variable loadings. In PLSC, the first dimension is extracted such that the pair of latent variables are as similar as possible, as measured by their covariance; this covariance is quantified by the first *singular value* of PLSC. Subsequently, the latent variables of the second dimension are obtained from the residual data of the first dimension and explain the maximum covariance from the residual data with this covariance stored as the second singular value. Subsequent dimensions are obtained in the same way. Together, PLSC dimensions explain the covariance of the data tables in a descending order and are orthogonal to each other. Given such orthogonality, these dimensions explain independent sources of covariance, and the squared singular values (i.e., the *eigenvalues*, denoted by λ) are thus additive. Specifically, they add up to the total squared scaled correlation of the two data tables, and the ratio of each eigenvalue with respect to this total quantifies the proportion of scaled correlation explained by each dimension (denoted by τ). As τ is similar to the idea of a proportion of variance explained as measured by η^2, τ can be interpreted as the effect size of a PLSC dimension.

Identify reliable dimensions. To identify reliable dimensions, we performed a permutation test on the singular values to determine if the covariance between the corresponding pair of latent variables are reliably larger than 0. In the permutation test, we first permuted the participants within each variable of both tables such that the relationships between them were null. The permuted tables were then analyzed by PLSC to extract the first singular value. This procedure was repeated 1000 times to generate the null distribution of the first singular value. For the second dimension, the first dimension was first regressed out from the data before the 1000 iterations of permutation and PLSC to obtain the null distribution of the second singular value; a similar procedure was used for subsequent dimension. Just like in the null hypothesis testing, we then compared the observed values to their corresponding null distribution and obtained their p value as the probability associated with each observed value under their null. A singular value with $p < .05$ indicates a reliable dimension ($\alpha = .05$).

Identify important variables and reliable loadings. To identify important variables for a given dimension, we quantified the *contribution* of each variable by computing the ratio of its squared loading to the eigenvalue. Because each variable was first normalised to have a sum of squares of 1, it originally contributed $1/J$ of variance to the total variance of the data table (with J being the number of variables). A contribution larger than $1/J$ therefore marks an important variable as it contributes more than average to the variance of a given dimension.

To identify reliable loadings, we used bootstrap tests to estimate the stability of the loadings. The bootstrap procedure generates a sampling distribution of the given measure (here, the loadings) assuming that the current sample is the best approximate of the population. Therefore, the bootstrap procedure generates subsamples from the original data set to estimate how the given measure varies. In the bootstrap procedure of PLSC, the participants were resampled with replacement to reconstruct the two resampled data tables. These two tables were centred by the original variable means and normalised by the original variable sums of squares then analysed by a PLSC to generate the loadings. This procedure was repeated 1000 times to generate the bootstrapped sampling distribution of all loadings. The reliability was then quantified by the *bootstrap ratio* (BR), which was computed by dividing each loading by the standard deviation of its bootstrapped sample distribution. Mathematically, BR is a *Z*-approximate that indicates whether the observed loading is reliably different from 0. Therefore, just like the Z test, a BR of 1.96 was used as the critical value to indicate reliability at α of .05. In this paper, regarding the excessive number of tests, we used a more stringent critical value of 2.88 for two-tail *Z* tests at $\alpha < .005$.

	Correlation with Cognitive Scores		Correlation with Brain Scores	
	r [95% CI]	*q*(FDR)	*r* [95% CI]	*q*(FDR)
Birchwood Social Functioning Scale (BSFS)	.14 [-.27, -.01]	.044	-.18 [-.3, -.05]	.014
Quality of Life Scale (QLS)	-.32 [-.43, -.19]	< .001	-.25 [-.37, -.12]	.001
Brief Psychiatric Rating Scale (BPRS)	.08 [-.05, .21]	.26	.05 [-.08, .18]	.466
Scale for the Assessment of Negative Symptoms (SANS)	.19 [.06, .31]	.01	.21 [.08, .33]	.004

Note: Two participants with missing values for QLS and two participants with missing values for SANS are removed from the analysis.

Table S1.

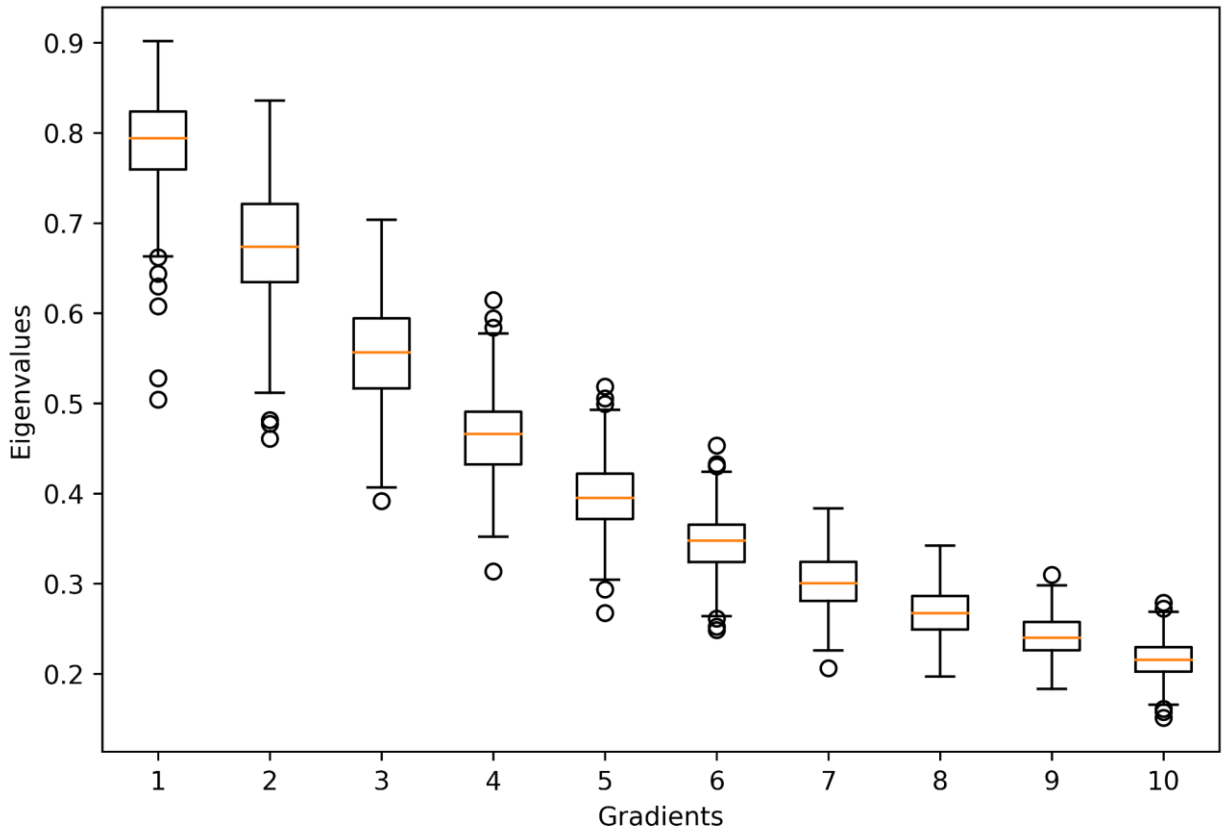

Figure S2. Boxplots of the eigenvalues from the first 10 dimensions extracted by the gradient analysis.

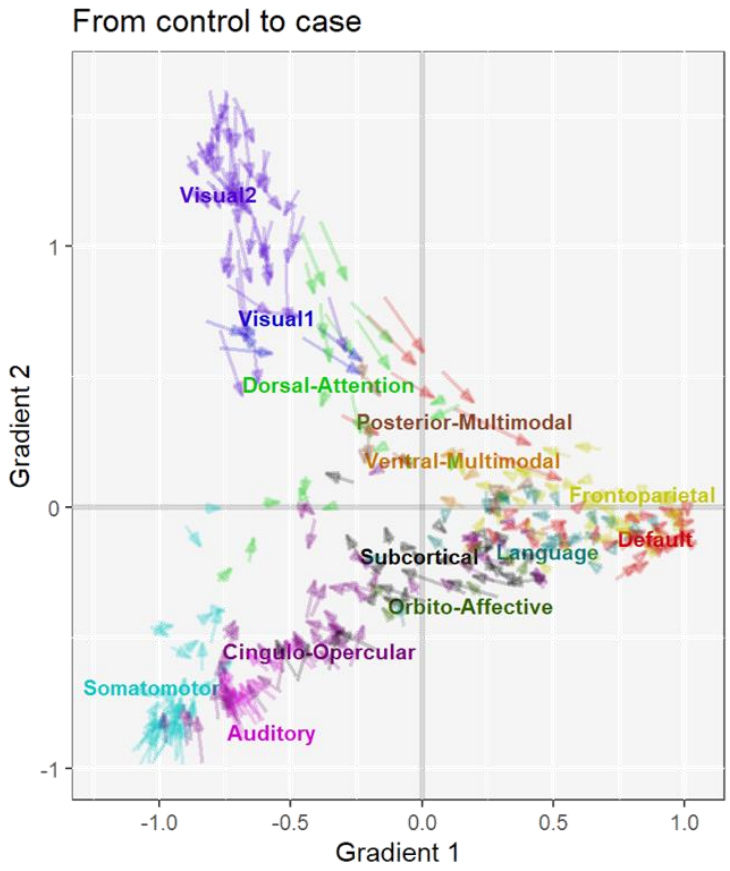

Figure S3. The scatter plot illustrates the group differences of each brain region on Gradients 1 and 2. In this plot, each arrow represents a region of interest (ROI) pointing from the mean gradient scores of the Control group to that of the SSD group. These arrows are colored by networks according to the Cole-Anticevic cortical atlas with the labels positioned at the mean gradient scores of each network. Specifically, this figure shows how ROIs from the default mode network (DMN), as compared to other networks, have decreased within-network, rather than between-network, segregation in SSD as all red arrows are pointing towards the network mean.

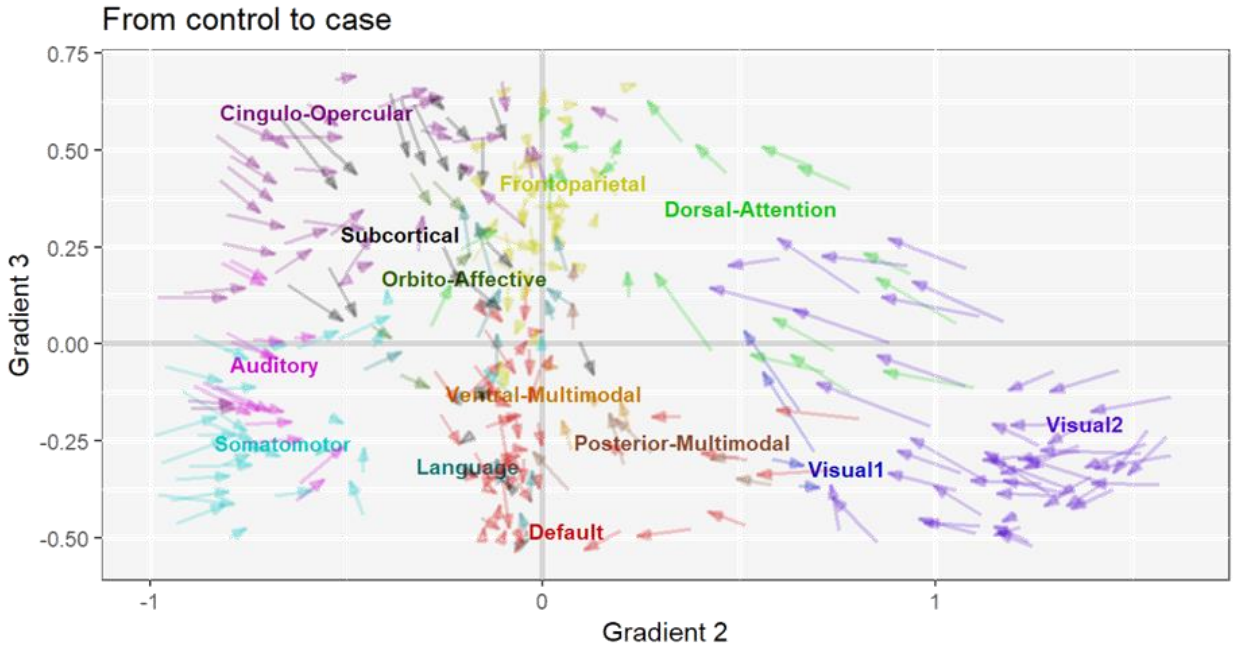

Figure S4. The scatter plot illustrates the group differences of each brain region on Gradients 2 and 3. In this plot, each arrow represents a region of interest (ROI) pointing from the mean gradient scores of the Control group to that of the SSD group. These arrows are colored by networks according to the Cole-Anticevic cortical atlas with the labels positioned at the mean gradient scores of each network. Specifically, this figure shows how ROIs from the default mode network (DMN), as compared to other networks, have decreased within-network, rather than between-network, segregation in SSD as all red arrows are pointing towards the network mean.

References

1. Chavez S, Viviano J, Zamyadi M, Kingsley PB, Kochunov P, Strother S, Voineskos A (2018): A novel DTI-QA tool: Automated metric extraction exploiting the sphericity of an agar filled phantom. *Magn Reson Imaging* 46: 28–39.
2. Hawco C, Viviano JD, Chavez S, Dickie EW, Calarco N, Kochunov P, *et al.* (2018): A longitudinal human phantom reliability study of multi-center T1-weighted, DTI, and resting state fMRI data. *Psychiatry Res Neuroimaging* 282: 134–142.
3. Kochunov P, Dickie EW, Viviano JD, Turner J, Kingsley PB, Jahanshad N, *et al.* (2018): Integration of routine QA data into mega-analysis may improve quality and sensitivity of multisite diffusion tensor imaging studies. *Hum Brain Mapp* 39: 1015–1023.
4. Viviano JD, Buchanan RW, Calarco N, Gold JM, Foussias G, Bhagwat N, *et al.* (2018): Resting-State Connectivity Biomarkers of Cognitive Performance and Social Function in Individuals With Schizophrenia Spectrum Disorder and Healthy Control Subjects. *Biol Psychiatry* 84: 665–674.
5. Esteban O, Markiewicz CJ, Blair RW, Moodie CA, Isik AI, Erramuzpe A, *et al.* (2019): fMRIPrep: a robust preprocessing pipeline for functional MRI. *Nat Methods* 16: 111–116.
6. Gorgolewski K, Burns CD, Madison C, Clark D, Halchenko YO, Waskom ML, Ghosh SS (2011): Nipype: A Flexible, Lightweight and Extensible Neuroimaging Data Processing Framework in Python. *Front Neuroinformatics* 5. https://doi.org/10.3389/fninf.2011.00013
7. Zhang Y, Brady M, Smith S (2001): Segmentation of brain MR images through a hidden Markov random field model and the expectation-maximization algorithm. *IEEE Trans Med Imaging* 20: 45–57.
8. Dale AM, Fischl B, Sereno MI (1999): Cortical Surface-Based Analysis. *NeuroImage* 9: 179–194.
9. Treiber JM, White NS, Steed TC, Bartsch H, Holland D, Farid N, *et al.* (2016): Characterization and Correction of Geometric Distortions in 814 Diffusion Weighted Images ((J. Najbauer, editor)). *PLOS ONE* 11: e0152472.
10. Jenkinson M, Bannister P, Brady M, Smith S (2002): Improved Optimization for the Robust and Accurate Linear Registration and Motion Correction of Brain Images. *NeuroImage* 17: 825–841.
11. Dickie EW, Anticevic A, Smith DE, Coalson TS, Manogaran M, Calarco N, *et al.* (2019): Ciftify: A framework for surface-based analysis of legacy MR acquisitions. *NeuroImage* 197: 818–826.
12. Glasser MF, Sotiropoulos SN, Wilson JA, Coalson TS, Fischl B, Andersson JL, *et al.* (2013): The minimal preprocessing pipelines for the Human Connectome Project. *NeuroImage* 80: 105–124.
13. Robinson EC, Jbabdi S, Glasser MF, Andersson J, Burgess GC, Harms MP, *et al.* (2014): MSM: A new flexible framework for Multimodal Surface Matching. *NeuroImage* 100: 414–426.
14. Krishnan A, Williams LJ, McIntosh AR, Abdi H (2011): Partial Least Squares (PLS) methods for neuroimaging: a tutorial and review. *Neuroimage* 56: 455–475.